Progress in Nuclear Energy 158 (2023) 104611



Contents lists available at ScienceDirect

Progress in Nuclear Energy

journal homepage: www.elsevier.com/locate/pnucene

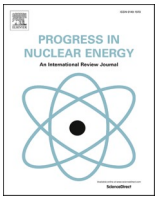



Drift-flux model for upward dispersed two-phase flows in vertical medium-to-large round tubes

Takashi Hibiki [a,*], Naofumi Tsukamoto [b]

[a] Department of Mechanical Engineering, City University of Hong Kong, 83 Tat Chee Avenue, Kowloon Tong, Hong Kong
[b] Regulatory Standard and Research Department, Secretariat of Nuclear Regulation Authority, Roppongi First Building, 1-9-9 Roppongi, Minato-ku, Tokyo, 106-8450, Japan

ARTICLE INFO

Keywords:
Drift-flux model
Drift velocity
Void fraction
Interfacial drag force
Interfacial heat transfer

ABSTRACT

The void fraction prediction is critical in nuclear safety analyses. Available one-dimensional computational codes heavily depend on the two-fluid model. The interfacial drag force in the momentum equation of the two-fluid model is currently formulated using the drift-flux model. Thus, the drift-flux model is critical for advanced two-phase flow analysis computational codes. The drift-flux model is characterized by two essential parameters: the distribution parameter and the drift velocity. The distribution parameter expresses the covariance of the area-averaged product of a void fraction and mixture volumetric flux. Flow channel geometry is a significant factor affecting the distribution parameter. The drift velocity expresses the relative velocity between gas and liquid phases. A bubble shape regime affects the drift velocity. The bubble shape regime is susceptible to flow regime dependence on the bubble Reynolds number. Bubbles in a spherical or distorted particle regime (group-1 bubbles) dominate in bubbly flow at a low void fraction, whereas bubbles in a slug or cap bubble regime (group-2 bubbles) play a critical role in beyond-bubbly flow. Whether slug bubbles or cap bubbles appear depends on the channel size. Thus, flow channel size significantly affects the drift velocity. The drift velocity dynamically changes along the two-phase flow, transforming from bubbly to beyond-bubbly flows.

The present study first formulates the evolution process of the drift velocity using the two-bubble-group approach. A two-group-based formulation is simplified to model the drift velocity behavior at the bubbly-to-beyond-bubbly flow transition. A scheme is proposed to explicitly calculate the distribution parameter and drift velocity using operating parameters. A drift-flux correlation with the new drift velocity model is evaluated by 750 data collected from 8 different sources. Tested fluid systems are nitrogen-water, air-water, and steam-water systems. Flow channel diameter ranges from 0.0508 to 0.305 m. Test section height (L)-to-channel diameter (D) ratio L/D ranges from 9.41 to 130. Superficial gas velocity is changed from 0.0100 to 11.2 m/s, whereas superficial liquid velocity is changed from 0 (pool condition) to 2.6 m/s. Operating pressure covers from 0.1 to 4.6 MPa. A systematic evaluation demonstrates the validity of the newly developed drift velocity model for a wide range of test conditions. This model is simple enough to be implemented into existing one-dimensional computational codes without any substantial code architecture change.

1. Introduction

Two-phase heat transfer analyses are critical in various industrial equipment designs, performance evaluations, and safety assessments. Two-phase flows are categorized into one-component and two-component two-phase flows. One-component two-phase flows, such as steam-water mixture flows, are formed due to phase change, whereas two-component two-phase flows, such as natural gas-oil mixture flows, are generated by mixing two immiscible components. The industrial equipment for two-phase heat transfer includes heat exchangers, condensers, boilers, steam generators, nuclear reactors, petroleum pipelines, etc.

Wall heat transfer for one-component two-phase flows is efficient due to heat transfer through wall nucleation and forced convection. Wall heat transfer for two-component two-phase flows is enhanced by steepening the temperature gradient at the wall, and the gradient is driven by the liquid velocity accelerated by the gas phase. Interfacial heat transfer between gas and liquid phases occurs due to the temperature difference between gas and liquid phases and is determined by the

* Corresponding author.
E-mail address: thibiki@cityu.edu.hk (T. Hibiki).

https://doi.org/10.1016/j.pnucene.2023.104611
Received 26 November 2022; Received in revised form 6 February 2023; Accepted 12 February 2023
Available online 22 February 2023
0149-1970/© 2023 The Authors. Published by Elsevier Ltd. This is an open access article under the CC BY license (http://creativecommons.org/licenses/by/4.0/).

Nomenclature

A	coefficient [-]
B	exponent [-]
C_e	coefficient [-]
C_0	distribution parameter [-]
D	round tube diameter [m]
D_{base}	cap bubble base diameter [m]
D_c	critical diameter of a maximum cap bubble [m]
D_H	hydraulic equivalent diameter [m]
D_{Sm}	bubble Sauter mean diameter [m]
$f(\langle\alpha\rangle)$	function of void fraction [-]
g	gravitational acceleration [m/s^2]
j	mixture volumetric flux [m/s]
j_f	superficial liquid velocity [m/s]
j_g	superficial gas velocity [m/s]
L	test section length [m]
La	Laplace length [m]
m_d	mean absolute error [-] or [m/s]
m_{rel}	mean relative deviation [-]
N	number of data [-]
$N_{\mu f}$	viscosity number for liquid phase [-]
N_ρ	density ratio [-]
s_d	standard deviation [-] or [m/s]
s_{rel}	standard relative deviation [-] or [m/s]
v_g	gas velocity [m/s]
v_{gj}	drift velocity [m/s]

Greek symbols

α	void fraction [-]
$\Delta\rho$	density difference between gas and liquid phases [kg/m^3]
ξ	linear ramp function [-]
ρ_f	liquid density [kg/m^3]
ρ_g	gas density [kg/m^3]
σ	surface tension [N/m]
ψ	value [-] or [m/s]

Mathematical symbols

$\langle\rangle$area-averaged quantity

$\langle\langle\rangle\rangle$void fraction-weighted mean quantity

Superscripts

$+$	parameter non-dimensionalized by $(\Delta\rho g\sigma/\rho_f^2)^{0.25}$
$*$	parameter non-dimensionalized by Laplace length

Subscripts

B	bubbly flow
cal	calculated value
crit	critical value expressing the boundary at medium-to-large-size channels
CT	churn-turbulent flow
exp.	measured value
i	i-th data
KI	value calculated by Kataoka and Ishii's correlation
n	n-th group
1	group-1
2	group-2

heat transfer coefficient and interfacial area concentration. The acceleration of the liquid velocity is characterized by the void fraction defined by the ratio of gas volume to control volume. The interfacial area concentration is geometrically related to the void fraction and bubble Sauter mean diameter. Therefore, accurate void fraction prediction is essential in two-phase heat transfer analyses.

The important role of computational fluid dynamics simulation codes for two-phase heat transfer analyses was discussed (Yeoh, 2019). These codes are classified into four categories depending on control volume size (or mesh size): one-dimensional analysis codes (Borkowski and Wade, 1992; Nuclear Regulatory Committee, U.S., 2008; Thermal Hydraulics Group, 1998); porous-media analysis codes (Carver et al., 1981; Komuro et al., 2022; Singhal et al., 1982); subchannel analysis codes (Hotta et al., 2004; Moorthi et al., 2018; Salko et al., 2019); and three-dimensional analysis codes (ANSYS, 2017; Sharma et al., 2017a, 2017b). Among them, Eulerian-Eulerian one-dimensional analysis codes are often used for thermo-fluid system simulations. All the above-mentioned codes require mass, momentum, and energy conservation equations. The two-fluid model accurately formulates mass, momentum, and energy conservation equations (Ishii and Hibiki, 2011); however, interfacial transfer terms for mass, momentum, and energy should be given as constitutive equations to close the mathematical system of the two-fluid model. The interfacial momentum transfer term significant for predicting void fraction is given as the interfacial drag force term.

The interfacial drag force term is generally formulated by the drag coefficient, interfacial area concentration, liquid density, and relative velocity between gas and liquid phases (Brooks et al., 2012a; Khan et al., 2000). Since an accurate prediction method of the interfacial area concentration was not available in the 1980s, Andersen and Chu (1983) proposed an alternative approach to eliminate the interfacial area concentration in the interfacial drag force term. The alternative method uses the drift-flux model (Zuber and Findlay, 1965) to formulate the interfacial drag force term with drift-flux parameters, such as distribution parameter and drift velocity. The distribution parameter expresses the deviation of phase and velocity distributions from uniform distributions, whereas the drift velocity expresses the difference between gas velocity and mixture volumetric flux. The drift-flux model successfully considers the kinematic non-equilibrium, such as the relative velocity between gas and liquid phases.

The distribution parameter is determined by assuming void fraction and mixture volumetric flux distributions. Assuming power-law distributions of void fraction and mixture volumetric flux for two-phase flows in round tubes analytically yields the distribution parameter of about 1.2 (Ishii, 1977). However, the simple analytical approach is not applicable to complicated channel geometries, high-pressure systems, subcooled flow conditions, etc. (Hibiki, 2019; Hibiki et al., 2022; Hibiki and Ishii, 2002a). Thus, an empirical approach using the density ratio between gas and liquid phases is often employed to obtain the constitutive equation for the distribution parameter.

Drift velocity is modeled by a drag force acting on a gas phase and takes different forms, depending on flow regimes (Ishii, 1977). The modeled constitutive equations for the drift velocity are generally discontinuous at flow regime boundaries. A physically-sound transition model is indispensable to the code architecture to ensure no discontinuity between flow regime boundaries. The drift velocity model applicable to the transition between bubbly to beyond-bubbly flows is critical because the interfacial area concentration takes its maximum value at the transition point between bubbly and beyond-bubbly flows. The void fraction prediction around the transition point is essential for the optimized design of chemical reactors.

From the above viewpoints, the present study aims at developing the drift velocity model applicable to the transition between bubbly and beyond-bubbly flows. The modeled drift velocity is employed for developing a robust drift-flux correlation for upward gas-liquid dispersed two-phase flows in vertical round tubes. The developed

drift-flux correlation is a powerful equation that can be implemented in thermal-system simulation codes to enhance the void fraction and mixture velocity prediction accuracy.

2. Drift-flux model and key constitutive equations

2.1. One-dimensional drift-flux model

The kinematic non-equilibrium in two-phase flow analyses is considered through the concept of the drift velocity v_{gj} (Zuber and Findlay, 1965). The drift velocity is defined as the difference between gas velocity v_g and mixture volumetric flux j.

$$v_{gj} = v_g - j. \tag{1}$$

The one-dimensional drift-flux model is obtained by area-averaging Eq. (1) as:

$$\langle\langle v_g \rangle\rangle = C_0 \langle j \rangle + \langle\langle v_{gj} \rangle\rangle, \tag{2}$$

where $\langle\,\rangle$ and $\langle\langle\,\rangle\rangle$ indicate the area-averaged and void fraction-weighted mean quantities, respectively. The distribution parameter C_0 is defined by:

$$C_0 \equiv \frac{\langle \alpha j \rangle}{\langle \alpha \rangle \langle j \rangle}. \tag{3}$$

The void fraction-weighted mean drift velocity is defined as:

$$\langle\langle v_{gj} \rangle\rangle \equiv \frac{\langle \alpha v_{gj} \rangle}{\langle \alpha \rangle}. \tag{4}$$

Equation (2) is non-dimensionalized by using the velocity scale $(\Delta\rho g\sigma/\rho_f^2)^{0.25}$ as follows:

$$\langle\langle v_g^+ \rangle\rangle = C_0 \langle j^+ \rangle + \langle\langle v_{gj}^+ \rangle\rangle, \tag{5}$$

where

$$\langle\langle v_g^+ \rangle\rangle \equiv \frac{\langle\langle v_g \rangle\rangle}{\left(\frac{\Delta\rho g\sigma}{\rho_f^2}\right)^{0.25}}, \tag{6}$$

$$\langle j^+ \rangle \equiv \frac{\langle j \rangle}{\left(\frac{\Delta\rho g\sigma}{\rho_f^2}\right)^{0.25}}, \tag{7}$$

$$\langle\langle v_{gj}^+ \rangle\rangle \equiv \frac{\langle\langle v_{gj} \rangle\rangle}{\left(\frac{\Delta\rho g\sigma}{\rho_f^2}\right)^{0.25}}. \tag{8}$$

Here, $\Delta\rho$, g, σ, and ρ_f are the density difference between gas and liquid phases, gravitational acceleration, surface tension, and liquid density, respectively.

2.2. Key constitutive equations

Ishii (1977) developed key constitutive equations of the drift velocity for vertical upward dispersed two-phase flows.

Bubbly flow:

$$\langle\langle v_{gj}^+ \rangle\rangle = \sqrt{2}(1 - \langle\alpha\rangle)^{1.75}. \tag{9}$$

Slug flow:

$$\langle\langle v_{gj}^+ \rangle\rangle = 0.35 {D_H^*}^{0.5}. \tag{10}$$

The non-dimensional flow channel size is defined by:

$$D_H^* \equiv \frac{D_H}{La}, \tag{11}$$

where D_H is the hydraulic equivalent diameter. Laplace length scale La is defined by:

$$La \equiv \left(\frac{\sigma}{\Delta\rho g}\right)^{0.5}. \tag{12}$$

Churn flow:

$$\langle\langle v_{gj}^+ \rangle\rangle = \sqrt{2}. \tag{13}$$

Ishii (1977) developed the constitutive equations of the distribution parameter for vertical upward dispersed two-phase flows as:

$$C_0 = 1.2 - 0.2 N_\rho^{0.5} \tag{14}$$

The density ratio N_ρ is defined by ρ_g/ρ_f, where ρ_g is the gas density. Kataoka and Ishii (1987) mentioned that the above drift-flux correlations are applicable to forced convective two-phase flows in medium size tubes with $D_H^* \le 40$.

Equation (14) is modified for subcooled boiling flows as:

$$C_0 = \left(1.2 - 0.2 N_\rho^{0.5}\right)\left(1 - e^{-18\langle\alpha\rangle}\right). \tag{15}$$

Hibiki and Ishii (2002a) further modified Eq. (14) for adiabatic bubbly flows where wall peaking in void fraction distribution is observed, depending on bubble size as:

$$C_0 = \left(1.2 - 0.2 N_\rho^{0.5}\right)\left(1 - e^{-22\frac{\langle D_{Sm}\rangle}{D_H}}\right), \tag{16}$$

where $\langle D_{Sm}\rangle$ is the bubble Sauter mean diameter. The bubble Sauter mean diameter for bubbly flows can be calculated by a correlation (Hibiki and Ishii, 2002b).

Kataoka and Ishii (1987) demonstrated that the above drift-flux correlations could not predict void fractions in large-size channels, particularly for $\langle j_g^+ \rangle > 0.5$. Ideal-shaped slug bubbles are formed in medium-size channels, whereas deformed large bubbles are formed in large-size channels. Kataoka and Ishii mentioned that the deformed large bubbles in large-size channels were characterized as cap bubbles rather than slug bubbles from the aspect of relative velocity between gas and liquid phases. The channel gap in a large-size channel is too large to stabilize slug bubbles. The large-cap bubbles are formed by the disintegration of the slug bubbles due to surface instability.

Other researchers investigated a cap bubble breakup criterion (Kitscha and Kocamustafaogullari, 1989; Kocamustafaogullari and Ishii, 1985). Those results demonstrated that no slug bubble could exist in a flow channel larger than the maximum bubble size deduced from the criterion. Brooks et al. (2012b) extended the criterion to formulate the drift velocity of large-cap bubbles. Kataoka and Ishii (1987) developed the criterion to estimate the critical non-dimensional flow channel size $D_{H,crit}^*$ where slug bubbles no longer exist.

$$D_{H,crit}^* = 30. \tag{17}$$

The flow channels with $D_H^* \ge 30$ and $D_H^* \le 30$ are categorized as large-size and medium-size channels, respectively.

Kataoka and Ishii (1987) developed the drift-flux correlation for the pool void fraction, focusing on large-size channels and high superficial gas velocity.

Low viscosity systems ($N_{\mu f} \le 2 \times 10^{-3}$):

$$\langle\langle v_{gj}^+ \rangle\rangle = 0.0019 {D_H^*}^{0.809} N_\rho^{-0.157} N_{\mu f}^{-0.562} \text{ for } D_H^* \le 30, \tag{18}$$

$$\langle\langle v_{gj}^+ \rangle\rangle = 0.030 N_\rho^{-0.157} N_{\mu f}^{-0.562} \text{ for } D_H^* \ge 30. \tag{19}$$

The viscosity number is defined by:

$$N_{\mu f} \equiv \frac{\mu_f}{\left(\rho_f \sigma La\right)^{0.5}}, \tag{20}$$

where μ_f is the kinematic viscosity of the liquid phase.

High viscosity systems ($N_{\mu f} \geq 2 \times 10^{-3}$):

$$\langle\langle v_{gj}^{+}\rangle\rangle = 0.92 N_{\rho}^{-0.157} \text{ for } D_{H}^{*} \geq 30. \quad (21)$$

It should be noted here that the constitutive equation for the drift velocity is not available for high viscosity systems with $D_{H}^{*} \leq 30$ due to lack of data.

Kataoka and Ishii (1987) discussed the effect of channel size on the distribution parameter. Although the channel height-to-size ratio and inlet conditions might affect the distribution parameter, they concluded that Eq. (14), which ignored the effects, might be approximately applicable to bubbling or pool boiling systems. In pool conditions, the order of magnitude of the first term on the right-hand side of Eq. (2) would be the same as that of the second term. Thus, the impact of the distribution parameter on the calculated void fraction might not be significant in comparison with forced convective flows with high $\langle j^{+}\rangle$. Kataoka and Ishii's drift-flux correlation was validated by extensive test conditions, such as superficial gas velocities from 0.1 to 2.5 m/s, channel diameters from 10 to 600 mm, and system pressures from 0.1 to 2.5 MPa for air-water systems and from 0.1 to 18.2 MPa for steam-water systems. The correlation could predict the void fraction within ±20%. Subsequent research also demonstrated the validity of Kataoka and Ishii's correlation over wide ranges of test conditions. Due to its reliability, Kataoka and Ishii's drift-flux correlation has been implemented in many one-dimensional analysis codes, such as the USNRC TRACE code (Nuclear Regulatory Committee, U.S., 2008).

Hills (1976), Shipley (1984), Clark and Flemmer (Clark and Flemmer, 1985, 1986), and Kawanishi et al. (1990) proposed purely empirical drift-flux correlations for large-size channels. Since the applicability of the correlations is limited due to their empirical nature, the current section does not discuss these correlations. It should be noted here that the above correlations developed for large-size channels are not applicable to medium-size channels.

3. Databases used in drift-flux modeling and validation

The detailed drift-flux modeling for dispersed two-phase flows requires complete sets of data for each data point, namely $\langle j_g\rangle$, $\langle j_f\rangle$, and $\langle\alpha\rangle$. The present study focuses on the data at the void fraction lower than 0.7, where the flow is characterized as a dispersed two-phase flow. Since the effect of the flow regime transition on the void fraction prediction is more pronounced in large-size channels, databases collected in large-size channels are selected. One database collected in a medium-size channel is also selected as a reference. This section briefly explains the databases selected for drift-flux modeling and validation.

3.1. The database of Hsu et al. (1998)

Fifty-one data were collected for vertical upward nitrogen-water dispersed two-phase flows in a 0.0508 m diameter round tube at Argonne National Laboratory. The height of the test section was 5.5 m. The gas phase was introduced into the test section through an injector comprised of 625 nozzles. Differential pressure transducers were used to measure the hydrostatic head of the two-phase flow. The measured differential pressure was converted to void fraction at low flow rates using the assumption of negligible frictional pressure drop. The test loop was operated for atmospheric pressure conditions. The data are not categorized as data in large-size channels. However, the data are important as reference data to discuss the difference in flow characteristics between medium and large-size channels.

3.2. The database of Hibiki and Ishii (2000a)

Fifty-nine data were collected for vertical upward nitrogen-water dispersed two-phase flows in a 0.102 m diameter round tube at Argonne National Laboratory. The height of the test section was 5.5 m. The gas phase was introduced into the test section through an injector comprised of 625 nozzles. Differential pressure transducers were used to measure void fraction at low flow rates due to negligible frictional pressure drop. The test loop was operated for atmospheric pressure conditions. The experiment was systematically conducted by changing superficial liquid velocity at a preset superficial gas velocity. The data collected at 9 different superficial gas velocity conditions were the best to characterize detailed two-phase flow behaviors, including the flow regime transition. The data are used for the drift-flux modeling to characterize the effect of flow parameters on drift velocity at the bubbly-to-beyond-bubbly flow transition in large-size channels. The rest of the data introduced in this section are used for independent validation of a new drift-flux correlation developed in the present study.

3.3. The database of Hills (1976)

Three hundred ninety-four data were collected for vertical upward air-water dispersed two-phase flows in a 0.149 m diameter round tube at the University of Nottingham. The height of the test section was 10.5 m. The gas phase was introduced into the test section through a 51 mm bore vertical tube. Void fraction was estimated by measured axial pressure difference and calculated frictional pressure loss using a correlation. The test loop was operated for atmospheric pressure conditions.

3.4. The database of Hashemi et al. (1986)

Forty data were collected for vertical upward air-water dispersed two-phase flows in a 0.305 m diameter round tube at the Electric Power Research Institute, Inc. The height of the test section was 2.88 m. The gas phase was introduced into the test section through a horizontal tube connected to a riser section. A single narrow-beam gamma densitometer was used to measure void fraction. The test loop was operated for atmospheric pressure conditions.

3.5. The database of Schlegel et al. (2014)

Fifty-five data were collected for vertical upward air-water dispersed two-phase flows in 0.152, 0.203, and 0.304 m diameter round tubes at Purdue University. The height of the test section was 4.4 m. The gas phase was introduced into the test section through an injector comprised of seven sparger units. Local void fractions were measured using a four-sensor probe. The area-averaged void fractions were calculated by integrating them over the flow channel and dividing them by the flow area. The test loop was operated for atmospheric pressure conditions.

3.6. The database of Shen et al. (2015)

One hundred sixteen data were collected for vertical upward air-water dispersed two-phase flows in a 0.200 m diameter round tube at the Japan Atomic Energy Agency. The height of the test section was 26 m. The gas phase was introduced into the test section through a porous ring tube injector composed of porous sinter tubes with circumferentially-aligned 2 × 80 holes each with a diameter of 0.5 mm. Differential pressure transducers were used to measure void fraction at low flow rates due to negligible frictional pressure drop. The test loop was operated for atmospheric pressure conditions.

3.7. The database of Omebere-Iyari et al. (2008)

Ten data were collected for vertical upward steam-water dispersed two-phase flows in a 0.194 m diameter round tube at Forschungszentrum Dresden-Rossendorf. The height of the test section was 9 m. The gas phase was introduced into the test section through a specially designed mixing section. The void fraction measurement was conducted using a wire-mesh sensor. The test loop was operated for the pressure P of 4.64 MPa.

Table 1
Databases used for new drift-flux correlation development.

References	Fluid Systems	D [m]	L/D [-]	Data No.	$<j_g>$ [m/s]	$<j_f>$ [m/s]	$<j>$ [m/s]	P [MPa]
Hsu et al. (1998)	N_2-Water	0.0508	108	51	0.0320–0.484	0.00–0.596	0.0320–1.02	0.1
Hibiki and Ishii, (2000a)	N_2-Water	0.102	53.9	59	0.0373–0.286	0.0109–0.387	0.0482–0.655	0.1
Hills, (1976) (Low Flow)	Air-Water	0.149	70.5	301	0.040–0.62	0.0–0.50	0.040–0.85	0.1
Hills, (1976) (High Flow)	Air-Water	0.149	70.5	93	0.10–3.5	0.0–2.6	0.10–6.1	0.1
Hashemi et al. (1986)	Air-Water	0.305	9.41	40	0.0100–1.16	0.0–0.060	0.0300–1.22	0.1
Schlegel et al. (2014) (6 inch diameter)	Air-Water	0.152	28.9	32	0.0462–11.2	0.245–1.75	0.256–11.9	0.1
Schlegel et al. (2014) (8 inch diameter)	Air-Water	0.203	21.7	9	0.207–4.13	0.268–0.913	0.447–4.42	0.1
Schlegel et al. (2014) (12 inch diameter)	Air-Water	0.304	14.5	14	0.215–2.33	0.235–0.466	0.515–2.79	0.1
Shen et al. (2015)	Air-Water	0.200	130	116	0.0178–0.211	0.0504–0.312	0.0731–0.812	0.1
Omebere-Iyari et al. (2008)	Steam-Water	0.194	46.4	10	0.109–0.949	0.100–0.650	0.278–1.59	4.6
Kawanishi et al. (1990)	Steam-Water	0.102	52.8	25	N/A	N/A	0.720–3.43	1.5

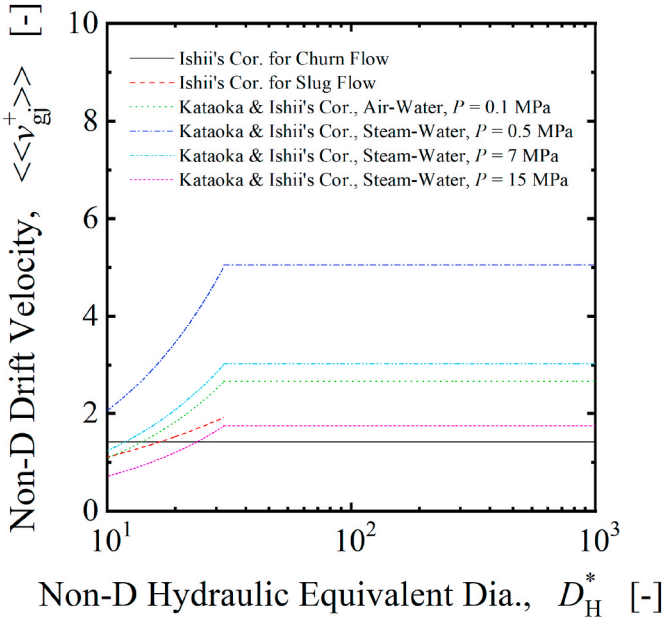

Fig. 1. Effects of channel diameter, flow regime, and pressure on non-dimensional drift velocity.

3.8. The database of Kawanishi et al. (1990)

Twenty-five data were collected for vertical upward steam-water dispersed two-phase flows in a 0.102 m diameter round tube at Mitsubishi Heavy Industries, Ltd. The height of the test section was 5.39 m. The gas phase was introduced into the test section through a sintered metal with many 20-μm holes in the mixing chamber. Electrical conductivity type void probes were used to measure void fraction. The test loop was operated for the pressure P of 1.5 MPa. The database does not provide complete sets of data for each data point, namely $\langle j_g \rangle$, $\langle j_f \rangle$, and $\langle \alpha \rangle$. However, since steam-water data at the high-pressure condition are limited, the data are considered in the analysis to examine the applicability of Kataoka and Ishii's correlation to high-pressure steam-water two-phase flows in the large-size channel.

3.9. Summary of test conditions

A total of 750 data are collected from eight different sources. The details of the test conditions are summarized in Table 1. The fluid systems used in the experiments are nitrogen-water, air-water, and steam-water systems. The flow channel diameter ranges from 0.0508 to 0.305 m. The test section height-to-channel diameter ratio L/D ranges from 9.41 to 130. The superficial gas velocity is changed from 0.0100 to 11.2 m/s, whereas the superficial liquid velocity is changed from 0 to 2.6 m/s. The operating pressure covers the range from 0.1 to 4.6 MPa.

4. Drift-flux model considering bubbly-to-beyond bubbly flow transition

4.1. Effects of flow conditions on drift velocity

Fig. 1 depicts the effects of flow conditions on drift velocity. The black solid and red dashed lines are the drift velocities calculated by Ishii's correlation for churn and slug flows, respectively. The drift velocity for slug flows is presented up to $D_H^+ = 30$, the threshold non-dimensional hydraulic equivalent diameter between medium and large-size channels. The green dotted, blue chain, cyan double chain, and magenta dotted lines are the drift velocities calculated by Kataoka and Ishii's correlation for air-water flows at $P = 0.1$ MPa, and steam-water flows at $P = 0.5$, 7, and 15 MPa, respectively.

Equating Eqs. (10) and (13) yields $D_H^* = 16.3$, where the drift velocities for slug and churn flows take the same values. The diameter for air-water flows under atmospheric and room temperature conditions is 0.0446 m. Under atmospheric and room temperature conditions, the non-dimensional drift velocities calculated by Ishii's correlations of churn flow and slug flow for air-water flow in a 0.0508 m ($D_H^* = 18.6$) round tube are 1.41 and 1.51, respectively. The non-dimensional drift velocity calculated by Kataoka and Ishii's correlation is 1.80. The non-dimensional drift velocities calculated by Ishii's correlations for churn flow and slug flow and Kataoka and Ishii's correlation are similar for air-water flow in a 0.0508 m round tube regardless of the flow regime.

Under atmospheric and room temperature conditions, the non-dimensional drift velocities calculated by Ishii's correlations of churn flow and slug flow for air-water flow in a 0.0819 m ($D_H^* = 30$) round tube are 1.41 and 1.97, respectively. The non-dimensional drift velocity calculated by Kataoka and Ishii's correlation is 2.66. Kataoka and Ishii's correlation calculates the non-dimensional drift velocity in a large-size channel with a much higher value than Ishii's correlations for churn flow and slug flow do. The difference is much magnified for steam-water flow. However, the difference is diminished as the pressure increases.

The above brief assessments lead to the following observations.

- The drift velocity for large-size channels is much underestimated if Ishii's correlation is used.
- The drift velocity effect on the void fraction prediction is significant at low mixture volumetric flux conditions, $C_0\langle j \rangle \sim \langle\langle v_{gj} \rangle\rangle$.
- The drift velocity effect is diminished as the mixture volumetric flux increases, $C_0\langle j \rangle \gg \langle\langle v_{gj} \rangle\rangle$.

4.2. Applicability of Kataoka and Ishii's correlation to forced convective flows

Kataoka and Ishii's correlation (Kataoka and Ishii, 1987) was developed for pool bubbling systems where the superficial liquid

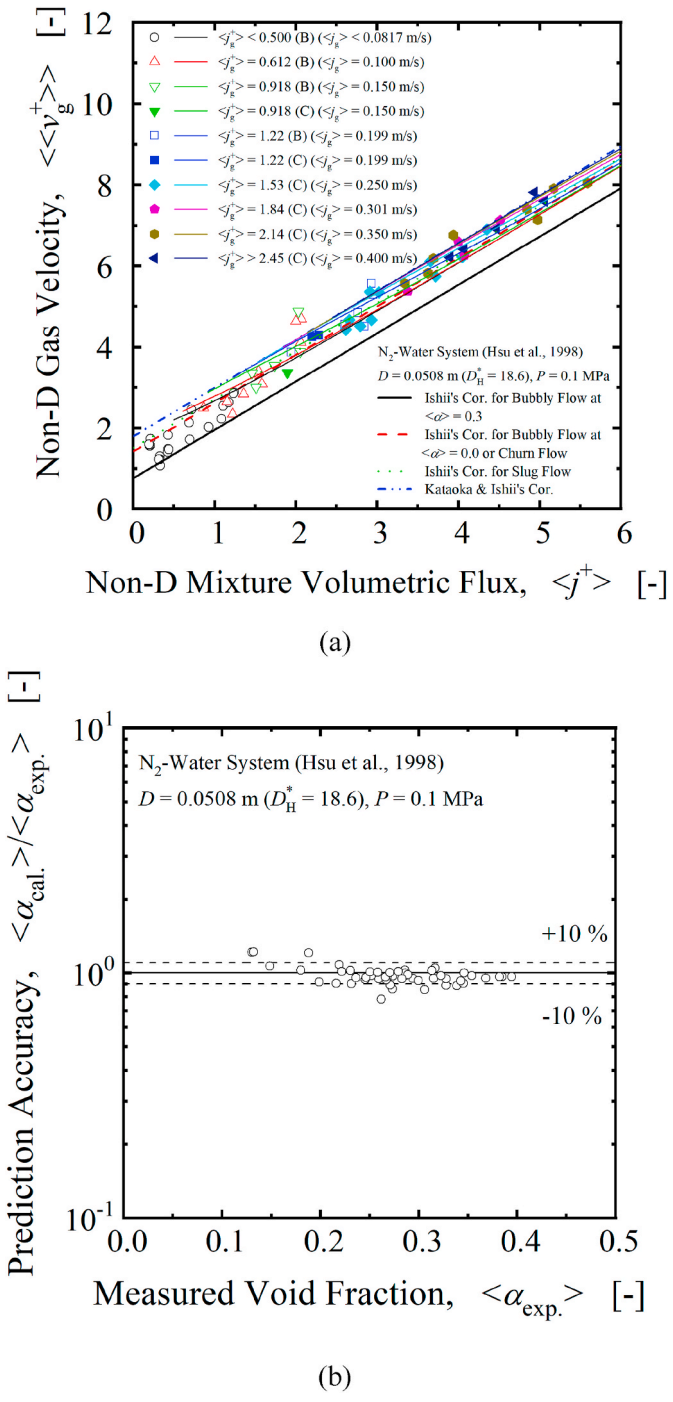

Fig. 2. Drift-flux plot (a) and new drift-flux correlation performance (b). The databases of Hsu et al. (1998) was used.

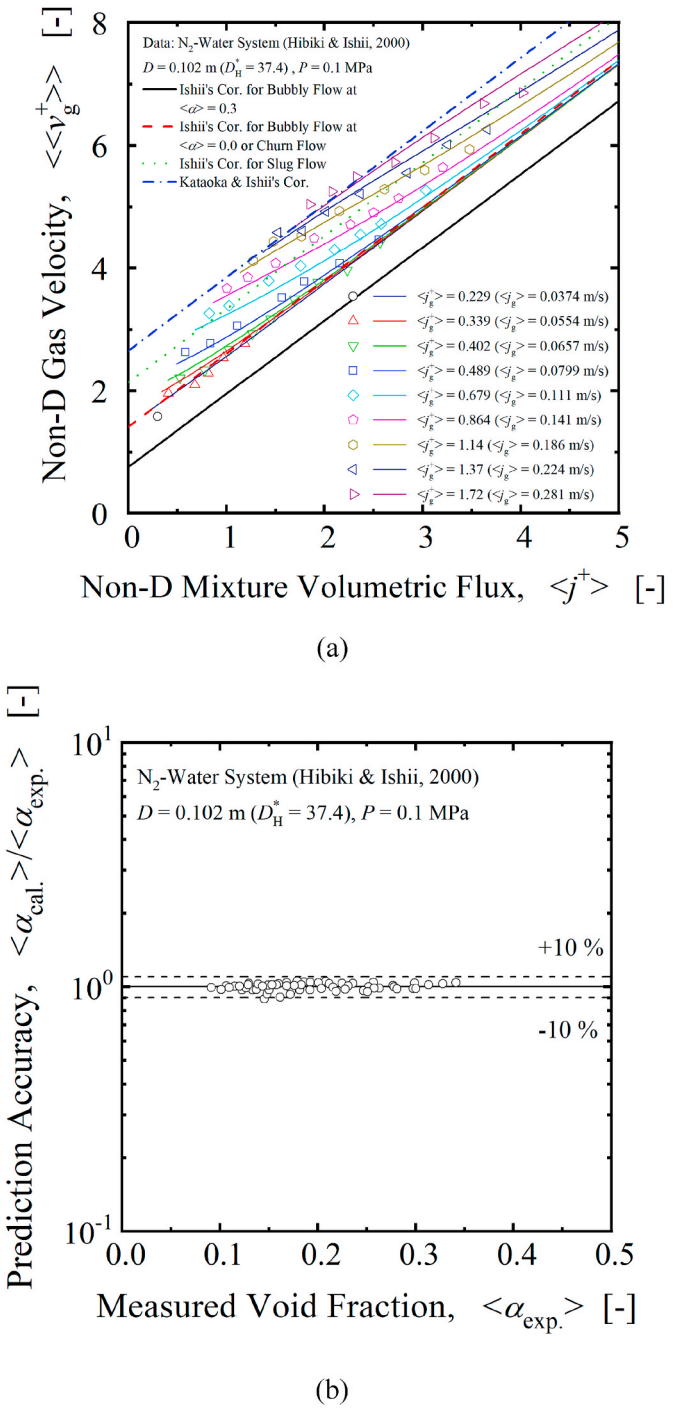

Fig. 3. Drift-flux plot (a) and new drift-flux correlation performance (b). The database of Hibiki and Ishii, (2000a) was used.

velocity was zero. This section examines the correlation's applicability to forced convective two-phase flows.

Fig. 2(a) shows the drift-flux plot for air-water flow in a 0.0508 m ($D_H^* = 18.6$) round tube under atmospheric and room temperature conditions. The channel size is categorized as a medium-size channel. The thick black solid, red dashed, green dotted, and blue chain lines are the values calculated by Ishii's correlation for bubbly flows at $\langle\alpha\rangle = 0.3$ and 0 (or churn flow), Ishii's correlation for slug flow, and Kataoka and Ishii's correlation, respectively. The thick black solid line provides the lower boundary of the gas velocity. Open and solid symbols are the data collected under conditions such that the gas phase is introduced into the test section as bubbly flow (B) and cap bubbly flow (C), respectively (Hibiki and Ishii, 2000a; Hsu et al., 1998). The effect of the inlet flow regime on the drift-flux plot is insignificant in the medium-size channel. When the superficial gas velocity is relatively low, the data are between the lines for bubbly flows at $\langle\alpha\rangle = 0$ and 0.3. As the superficial gas velocity increases, the data converges along the lines of slug flow and churn flow. Kataoka and Ishii's correlation overestimates the gas velocity at relatively low superficial gas velocity conditions. Kataoka and Ishii's correlation calculates the gas velocity reasonably well at higher superficial gas velocity conditions.

Fig. 3(a) shows the drift-flux plot for air-water flow data in a 0.102 m ($D_H^* = 37.4$) round tube under atmospheric and room temperature

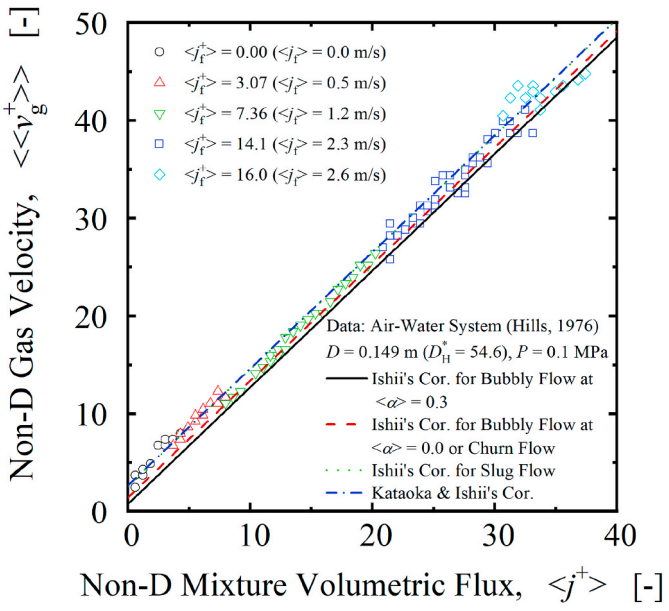

Fig. 4. Drift-flux plot for the database of Hills, (1976).

conditions (Hibiki and Ishii, 2000a). The channel size is categorized as a large-size channel. When the superficial gas velocity is relatively low, the data are between the lines for bubbly flows at $\langle\alpha\rangle = 0$ and 0.3. As the superficial gas velocity increases, the data start to deviate from the lines of bubbly flow and approach the line of Kataoka and Ishii's correlation. The flow regime transition from bubbly to beyond-bubbly (or cap bubbly) flows affects the drift velocity. Kataoka and Ishii's correlation overestimates the gas velocity but reasonably calculates the gas velocity at the highest superficial gas velocity condition, $\langle j_g^+\rangle = 1.72$.

Fig. 4 shows the drift-flux plot for air-water flow data in a 0.149 m ($D_H^* = 54.6$) round tube under atmospheric and room temperature conditions (Hills, 1976). The channel size is categorized as a large-size channel. Since the mixture volumetric flux is high, the impact of the drift velocity correlation on the drift-flux plot is insignificant, $C_0\langle j\rangle \gg \langle\langle v_{gj}\rangle\rangle$. Kataoka and Ishii's correlation and Ishii's correlation for churn flow reasonably predict the gas velocity.

Fig. 5(a) shows the drift-flux plot for steam-water flow data in a 0.102 m ($D_H^* = 47.9$) round tube under $P = 1.5$ MPa condition (Kawanishi et al., 1990). The channel size is categorized as a large-size channel. The data are scattered due to the measurement difficulty for the high-pressure condition. Ishii's correlation for bubbly, slug, and churn flows underestimates the gas velocity, whereas Kataoka and Ishii's correlation reasonably predicts the gas velocity.

The above brief experimental assessments lead to the following observations.

- The flow regime transition from bubbly to beyond-bubbly (cap bubbly) flows affects the drift velocity. The effect of the flow regime transition is more pronounced in large-size channels.
- Kataoka and Ishii's correlation does not predict the data in bubbly flows.
- Kataoka and Ishii's correlation reasonably predicts the data in beyond-bubbly flows.

4.3. Assessment of the existing drift velocity models at the transition between bubbly and beyond-bubbly flows

The TRACE code developed by the USNRC (Nuclear Regulatory Committee, U.S., 2008) handles the effect of flow regime transition on drift velocity using a simple linear ramp as:

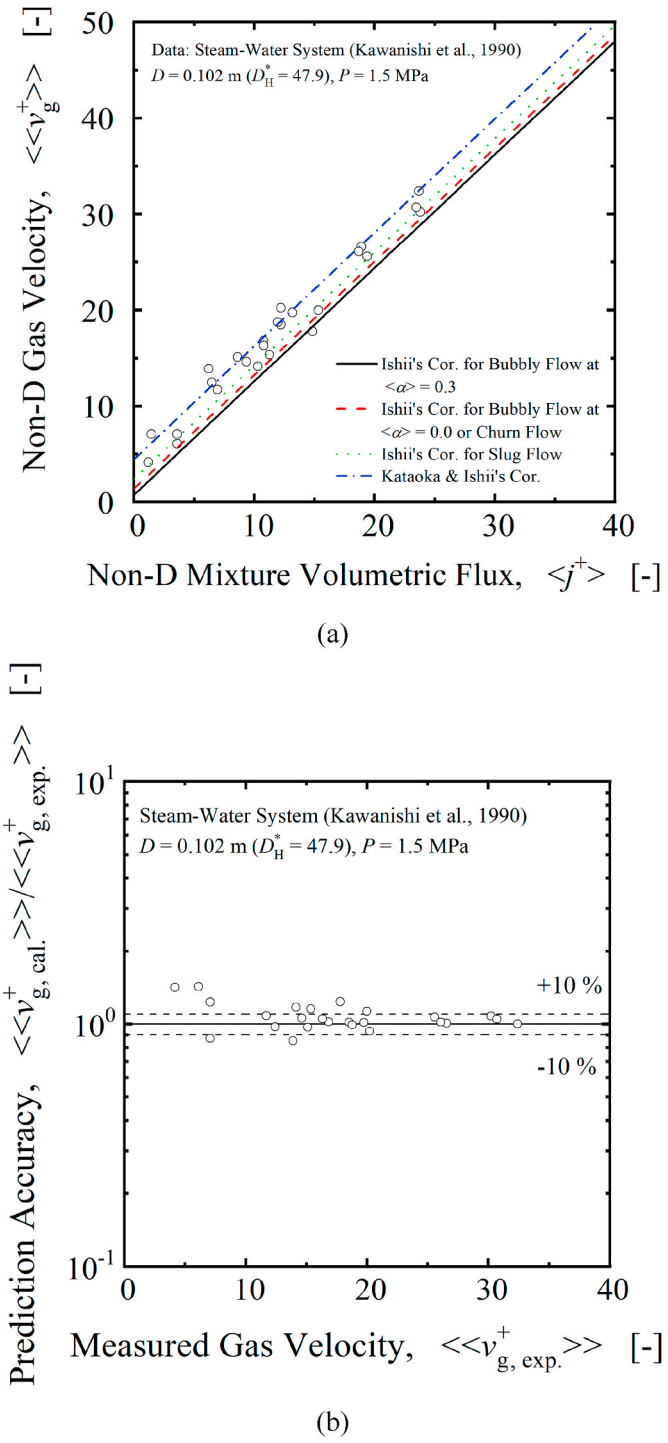

Fig. 5. Drift-flux plot (a) and new drift-flux correlation performance (b). The database of Kawanishi et al. (1990) was used.

$$\langle\langle v_{gj}^+\rangle\rangle = \langle\langle v_{gj,CT}^+\rangle\rangle\xi + \langle\langle v_{gj,KI}^+\rangle\rangle(1-\xi) \text{ for } 0.2 \le \langle\alpha\rangle \le 0.3, \tag{22}$$

where the subscripts CT and KI indicate the churn-turbulent flow correlation Eq. (13) and Kataoka and Ishii correlation, respectively. The linear ramp is given by:

$$\xi = \frac{0.3 - \langle\alpha\rangle}{0.3 - 0.2}. \tag{23}$$

The above simple linear ramp assumes that the flow regime transition between bubbly and beyond-bubbly flows occurs at the void

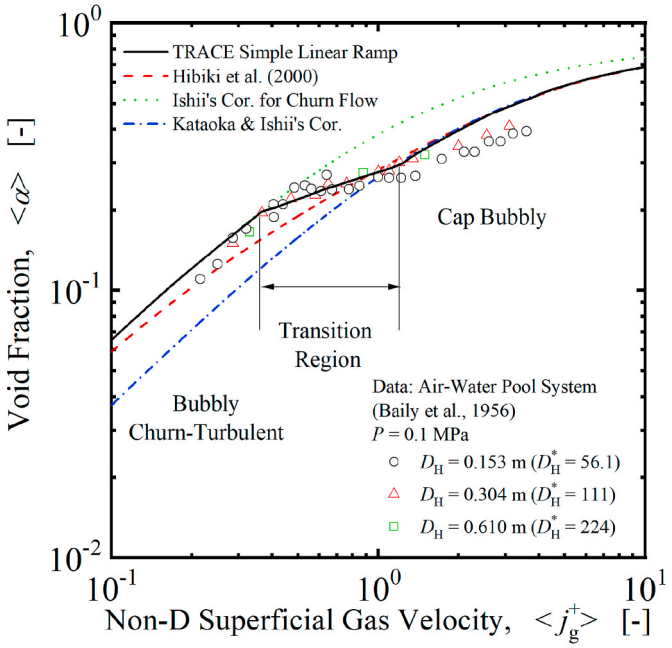

Fig. 6. Predictions of pool void fraction using drift velocity models at the transition between bubbly and beyond-bubbly flows.

fraction between 0.2 and 0.3.

Hibiki et al. (2000) considered Kataoka and Ishii's observation such that Ishii's drift velocity correlation was applicable to $\langle j_g^+ \rangle \leq 0.5$, and they proposed the drift velocity model at the transition between bubbly and beyond-bubbly flows as:

$$\langle\langle v_{gj}^+\rangle\rangle = \langle\langle v_{gj,CT}^+\rangle\rangle e^{-1.39\langle j_g^+\rangle} + \langle\langle v_{gj,KI}^+\rangle\rangle\left(1 - e^{-1.39\langle j_g^+\rangle}\right). \quad (24)$$

Hibiki and Ishii (2003) modified Eq. (24) as follows:

$$\langle\langle v_{gj}^+\rangle\rangle = \langle\langle v_{gj,B}^+\rangle\rangle e^{-1.39\langle j_g^+\rangle} + \langle\langle v_{gj,KI}^+\rangle\rangle\left(1 - e^{-1.39\langle j_g^+\rangle}\right), \quad (25)$$

where the subscript B indicates the bubbly flow correlation Eq. (9).

Fig. 6 compares the drift velocity models at the transition between bubbly and beyond-bubbly flow with data collected for air-water pool conditions (Baily et al., 1956). The black solid, red dashed, green dotted, and blue chain lines indicate the void fractions calculated by the TRACE model, Hibiki et al.'s model, Ishii's correlation for churn flow, and Kataoka and Ishii's correlation, respectively. Kataoka and Ishii's correlation underestimates the pool void fraction at low superficial gas velocity conditions due to the overestimated drift velocity. Ishii's correlation overestimates the pool void fraction at high superficial gas velocity conditions due to the underestimated drift velocity. The TRACE model and Hibiki et al.'s model reasonably predict the pool void fraction by capturing the drift velocity behavior at the transition between bubbly and beyond-bubbly flows.

The two models validated using the pool void fraction data are examined by forced convective flow data at low mixture volumetric flux conditions. The drift velocities are back-calculated by measured data of void fraction and mixture volumetric flux. Fig. 7(a) and **7(b)**, respectively, compare the TRACE model and Hibiki et al.'s model with data collected for forced convective air-water flow in a 0.102 m ($D_H^* = 37.4$) round tube under atmospheric and room temperature conditions (Hibiki and Ishii, 2000a). The black solid line indicates the values calculated by the models. The data in Fig. 7(a) suggest that the transition between bubbly and beyond-bubbly flows occurs at the void fraction smaller than 0.2. Hibiki and his colleagues (Hibiki et al., 2001; Hibiki and Ishii, 1999) observed that cap bubbles in forced convective bubbly flows started to form at the void fraction of 0.15. The TRACE model did not work for

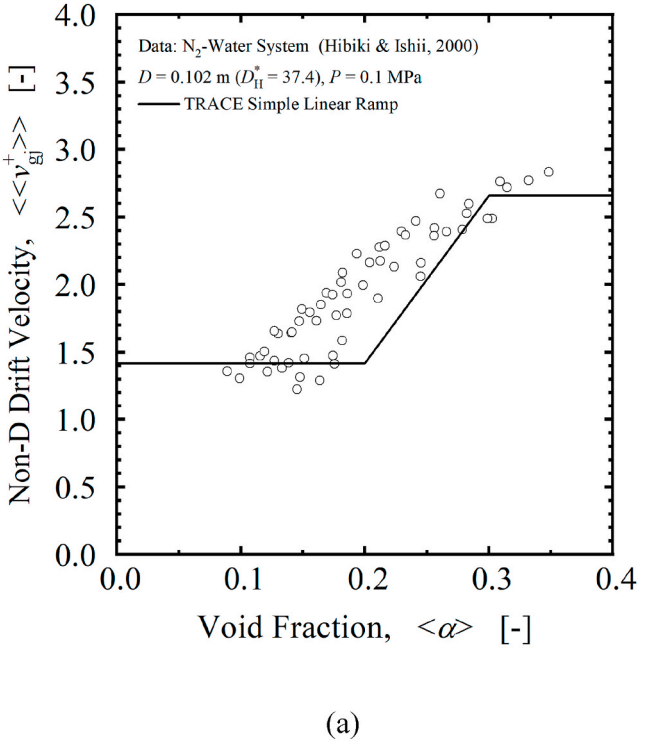

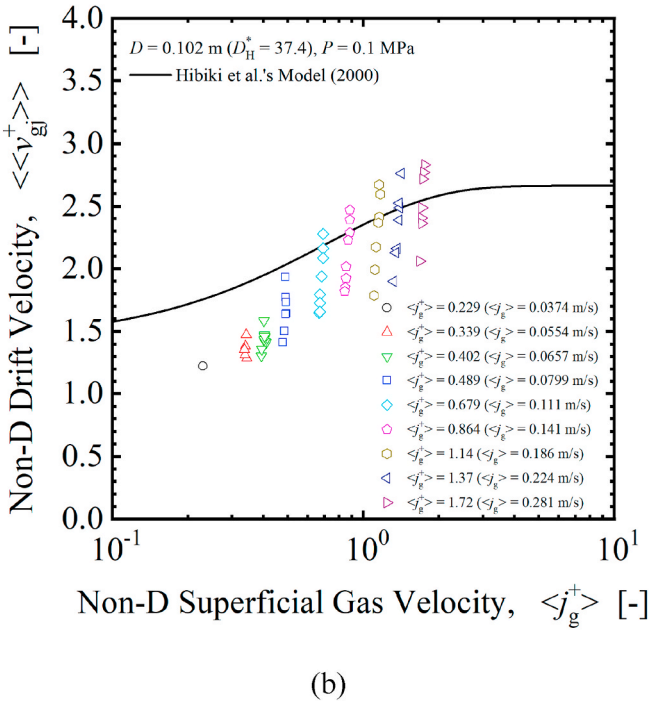

Fig. 7. Drift velocity models at the transition between bubbly and beyond-bubbly flows: TRACE model (a) and Hibiki et al.'s model (b).

steam and water data because the transition occurred at a much lower void fraction than that observed in air-water pool data (Nuclear Regulatory Committee, U.S., 2008). The observations are consistent with the results presented in Fig. 7(a). The TRACE model fails to reproduce the drift velocity variation at the transition between bubbly and cap-bubbly flows. Fig. 7(b) indicates that Hibiki et al.'s model fails to reproduce the drift velocity variation at the transition between bubbly and

beyond-bubbly flows. The non-dimensional superficial gas velocity may not be an appropriate parameter to model the drift velocity variation at the transition between bubbly and beyond-bubbly flows because the measured drift velocity takes different values at a fixed superficial gas velocity.

The above analyses indicate that the TRACE model and Hibiki et al.'s model should be revisited to develop an appropriate drift velocity model applicable to both pool and forced convective two-phase flow conditions.

4.4. Two-group approach in modeling drift velocity at the transition between bubbly and beyond-bubbly flows

The analyses presented in section 4.3 lead to some critical observations.

- The TRACE model and Hibiki et al.'s model reasonably calculate the variation of drift velocity at the transition between bubbly and beyond-bubbly flows for pool two-phase flows.
- The TRACE model and Hibiki et al.'s model fail to calculate the variation of drift velocity at the transition between bubbly and beyond-bubbly flows for forced convective two-phase flows.
- The non-dimensional superficial gas velocity is not an appropriate parameter to model the variation of drift velocity at the transition between bubbly and beyond-bubbly flows.
- The void fraction may be an appropriate parameter to model the variation of drift velocity at the transition between bubbly and beyond-bubbly flows. However, the onset of cap bubble formation occurs at a much lower void fraction than the value of 0.2 used in the TRACE model.
- Ishii's correlation for churn flow tends to overestimate the drift velocity for some flow conditions.

Bubbles in two-phase flows have a broad spectrum of bubble sizes. Bubbles are categorized into spherical, distorted, and cap (or slug) bubbles regarding transport characteristics or drag coefficient. Spherical or distorted bubbles appear in bubbly flow, whereas cap (or slug) bubbles dominate in cap bubbly (or slug) flow. The traditional drift-flux model proposed by Zuber and Findlay (1965) does not consider the difference in bubble transport characteristics. In other words, Zuber and Findlay treated bubbles as belonging to only one group. Multi-group approach considering a detailed spectrum of bubble sizes requires multi-group gas momentum equations, which are difficult to be solved numerically. Thus, a simple two-group approach is proposed to model the difference in bubble transport characteristics (Hibiki and Ishii, 2000b). The spherical and distorted bubbles dominant in bubbly flow are categorized as group-1 bubbles, whereas the cap and slug bubbles dominant in beyond-bubbly flow are categorized as group-2 bubbles. The two-group drift-flux model (Brooks et al., 2012b) is more mechanistic in characterizing the flow regime transition. The local drift velocity for group-n is defined by:

$$v_{\mathrm{gj,n}} \equiv v_{\mathrm{g,n}} - j, \tag{26}$$

where the subscript n denotes the bubble belonging to group-n. The non-dimensionalized form of the n-group drift-flux model is given by:

$$\langle\langle v^{+}_{\mathrm{g,n}}\rangle\rangle = C_{0,\mathrm{n}}\langle j^{+}\rangle + \langle\langle v^{+}_{\mathrm{gj,n}}\rangle\rangle, \tag{27}$$

where

$$C_{0,\mathrm{n}} \equiv \frac{\langle \alpha_{\mathrm{n}} j\rangle}{\langle \alpha_{\mathrm{n}}\rangle\langle j\rangle}, \tag{28}$$

$$\langle\langle v^{+}_{\mathrm{gj,n}}\rangle\rangle \equiv \frac{\langle \alpha_{\mathrm{n}} v^{+}_{\mathrm{gj,n}}\rangle}{\langle \alpha_{\mathrm{n}}\rangle}. \tag{29}$$

The distribution parameter in the traditional drift-flux model Eq.(3) is related to Eq. (28) as:

$$C_0 = C_{0,1}\frac{\langle \alpha_1\rangle}{\langle\alpha\rangle} + C_{0,2}\left(1 - \frac{\langle \alpha_1\rangle}{\langle\alpha\rangle}\right). \tag{30}$$

The drift velocity in the traditional drift-flux model Eq. (4) is also related to Eq. (29) as:

$$\langle\langle v^{+}_{\mathrm{gj}}\rangle\rangle = \langle\langle v^{+}_{\mathrm{gj,1}}\rangle\rangle\frac{\langle \alpha_1\rangle}{\langle\alpha\rangle} + \langle\langle v^{+}_{\mathrm{gj,2}}\rangle\rangle\left(1 - \frac{\langle \alpha_1\rangle}{\langle\alpha\rangle}\right). \tag{31}$$

The group-2 drift velocity $\langle\langle v^{+}_{\mathrm{gj,2}}\rangle\rangle$ is higher than the group-1 drift velocity $\langle\langle v^{+}_{\mathrm{gj,1}}\rangle\rangle$. Thus, the drift velocity $\langle\langle v^{+}_{\mathrm{gj}}\rangle\rangle$ beyond bubbly flow regime is higher than the group-1 drift velocity $\langle\langle v^{+}_{\mathrm{gj,1}}\rangle\rangle$ due to the formation of group-2 bubbles.

Brooks et al. (2012b) formulated the drift velocities for group-1 and group-2 bubbles as.

Group-1 bubbles:

$$\langle\langle v^{+}_{\mathrm{gj,1}}\rangle\rangle = \sqrt{2}(1 - \langle\alpha_1\rangle)^{1.75}. \tag{32}$$

Group-2 bubbles:

$$\langle\langle v^{+}_{\mathrm{gj,2}}\rangle\rangle = 0.54 {D^{*}_{\mathrm{base}}}^{0.5}(1 - \langle\alpha_2\rangle)^{1.5} \; for \; D_{\mathrm{base}} < D_{\mathrm{c}}, \tag{33}$$

$$\langle\langle v^{+}_{\mathrm{gj,2}}\rangle\rangle = 0.7 C_{\mathrm{e}}^{0.5}(1 - \langle\alpha_2\rangle)^{1.5} \; for \; D_{\mathrm{base}} = D_{\mathrm{c}}, \tag{34}$$

where D_{base} and D_{c} are the base diameter of a cap bubble and critical diameter of a maximum cap bubble, respectively. The non-dimensionalized base diameter of a cap bubble D_{base} is defined by:

$$D^{*}_{\mathrm{base}} \equiv \frac{D_{\mathrm{base}}}{La}. \tag{35}$$

The coefficient C_{e} is expressed by:

$$C_e = 27.1\left(1 + N_{\mu f}\right)^{0.83}. \tag{36}$$

The features of Eq. (31) are summarized as follows.

- When no group-2 bubble exists, Eq. (31) is reduced to the drift velocity for bubbly flow Eq. (32).
- The increase in void fraction decreases the drift velocity until group-2 bubbles are formed, see Eq. (32).
- When group-2 bubbles are formed, the increase in void fraction increases the drift velocity until the transition between bubbly and cap-bubbly flows is completed.
- When the flow regime transition is completed, the drift velocity becomes constant until the flow regime transition from dispersed to separate two-phase flows occurs.

Since the prediction method of $\langle\alpha_1\rangle$ (or $\langle\alpha_2\rangle$) in beyond-bubbly flow conditions has not been established, Eq. (31) may not be used for calculating the drift velocity. Thus, Eq. (31) is approximated by

$$\langle\langle v^{+}_{\mathrm{gj}}\rangle\rangle = \langle\langle v^{+}_{\mathrm{gj,B}}\rangle\rangle f(\langle\alpha\rangle) + \langle\langle v^{+}_{\mathrm{gj,KI}}\rangle\rangle(1 - f(\langle\alpha\rangle)), \tag{37}$$

where $f(\langle\alpha\rangle)$ is a function of $\langle\alpha\rangle$. Here, $\langle\langle v^{+}_{\mathrm{gj,B}}\rangle\rangle = \langle\langle v^{+}_{\mathrm{gj,1}}\rangle\rangle$. $\langle\alpha_1\rangle/\langle\alpha\rangle$ is approximated by a function of $\langle\alpha\rangle$. The value of function $f(\langle\alpha\rangle)$ should be one at $\langle\alpha\rangle = 0$ and asymptotically decreases zero as $\langle\alpha\rangle$ increases. Then, the drift velocity calculated by Eq. (37) is reduced to the drift velocity for bubbly flow (Eq. (32)).

The function $f(\langle\alpha\rangle)$ may take the following form with sufficient flexibility to model the flow regime transition behavior of the drift velocity:

$$f(\langle\alpha\rangle) = e^{A\langle\alpha\rangle^{B}}, \tag{38}$$

where A and B are constants.

The drift velocity modeled by Eqs. (37) and (38) is an implicit function of operating conditions $\langle j_{\mathrm{g}}\rangle$ and $\langle j_{\mathrm{f}}\rangle$ as:

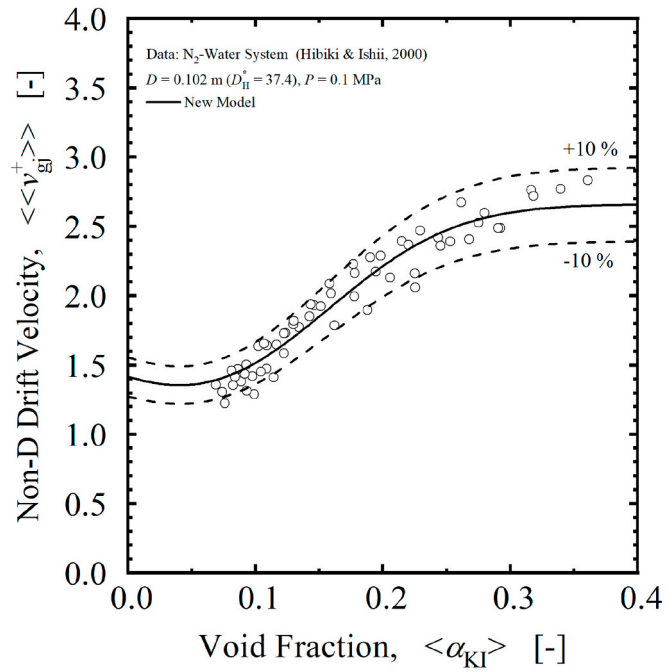

(a)

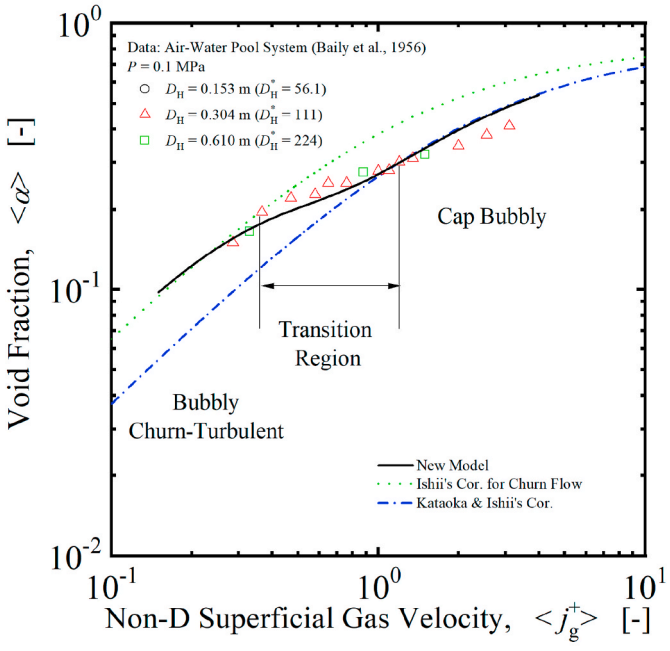

(b)

Fig. 8. New drift velocity model at the transition between bubbly and beyond-bubbly flows: forced convective two-phase flows and pool two-phase flows (b).

$$\langle\langle v_{gj}^{+}\rangle\rangle = \sqrt{2}(1-\langle\alpha\rangle)^{1.75}e^{A\langle\alpha\rangle^{B}} + \langle\langle v_{gj,KI}^{+}\rangle\rangle\left(1-e^{A\langle\alpha\rangle^{B}}\right). \tag{39}$$

Here, the void fraction in Eq. (39) is replaced by the void fraction $\langle\alpha_{KI}\rangle$ calculated by Kataoka and Ishii's correlation Eqs. (14) and (18)-(21) as:

$$\langle\langle v_{gj}^{+}\rangle\rangle = \sqrt{2}(1-\langle\alpha_{KI}\rangle)^{1.75}e^{A\langle\alpha_{KI}\rangle^{B}} + \langle\langle v_{gj,KI}^{+}\rangle\rangle\left(1-e^{A\langle\alpha_{KI}\rangle^{B}}\right). \tag{40}$$

Equation (40) allows for calculating the drift velocity with operating conditions explicitly. As demonstrated in section 4.2, Kataoka and Ishii's correlation is applicable to beyond-bubbly flow conditions. Although the prediction accuracy of Kataoka and Ishii's correlation deteriorates in bubbly flow at low mixture volumetric flux conditions, the deteriorated accuracy may not directly affect the prediction accuracy of the drift velocity for bubbly flow due to its functional dependence of $(1-\langle\alpha_{KI}\rangle)^{1.75}$. If the deviation between the true and calculated void fractions is 10%, the resultant effect on the drift velocity for bubbly flow is 3% at $\langle\alpha\rangle = 0.15$. If the deviation between the true and calculated void fractions is 20%, the resultant effect on the drift velocity is 6% at $\langle\alpha\rangle = 0.15$. The coefficients $A(=-60.63)$ and $B(=2.367)$ are experimentally determined using the data collected at the transition between bubbly and beyond-bubbly flows (Hibiki and Ishii, 2000a). The coefficients include the prediction deterioration of Kataoka and Ishii's correlation in bubbly flow at low mixture volumetric flux conditions.

Fig. 8(a) compares the drift velocity calculated by Eq. (40) with forced convective air-water flow data in a 0.102 m ($D_H^* = 37.4$) round tube under atmospheric and room temperature conditions (Hibiki and Ishii, 2000a). The black solid line indicates the calculated drift velocity. The drift velocity first decreases with the increase in void fraction. Then the drift velocity increases with the increase in void fraction due to the formation of cap bubbles. Finally, the drift velocity reaches a constant value when the transition between bubbly and beyond-bubbly flows is completed. The drift velocity for forced convective two-phase flow at the transition between bubbly and beyond-bubbly flows is predicted within ±10% by the new drift velocity model Eq. (40).

Fig. 8(b) examines the applicability of the new drift-flux correlation Eqs. (14) and (40) to two-phase flows in pool conditions. The new drift-flux correlation reasonably calculates the pool void fraction. As shown in Fig. 8(a) and (b), the assessment results indicate the validity of Eq. (40) for pool and forced convective two-phase flows.

4.5. Distribution parameter for subcooled boiling flows

The distribution parameter for subcooled boiling flows in a round tube is given by Eq. (15). The distribution parameter modeled by Eq. (15) is an implicit function of operating conditions $\langle j_g\rangle$ and $\langle j_f\rangle$. The void fraction in Eq. (15) is replaced with the void fraction $\langle\alpha_{CT}\rangle$ calculated by Ishii's correlation for churn flow Eqs. (13) and (14) as:

$$C_0 = \left(1.2-0.2N_\rho^{0.5}\right)\left(1-e^{-18\langle\alpha_{CT}\rangle}\right) \tag{41}$$

where

$$\langle\alpha_{CT}\rangle = \frac{\langle j_g^{+}\rangle}{\left(1.2-0.2N_\rho^{0.5}\right)\langle j^{+}\rangle + \sqrt{2}} \tag{42}$$

Fig. 9(a) compares results obtained using Eq. (15) with the data (Marchaterre, 1956; Maurer, 1956; St. Pierre, 1965) used in developing the equation (Ishii, 1977). Black solid lines are the distribution parameters calculated by Eq. (15) for different density ratios. The data indicated as black circles are significantly scattered around the lines obtained using Eq. (15). Fig. 9(b), (c), and 9(d) compare the distribution parameters calculated by Eq. (15) with the distribution parameters calculated by Eq. (41) for $\langle j_f\rangle = 0.00$, 1.0, and 2.0 m/s, respectively. Black solid, red dashed, green dotted, and blue chain lines are the distribution parameters calculated by Eq. (15) for steam-water two-phase flows under the pressures of 0.10, 1.0, 7.0, and 15 MPa, respectively. Black circles, red triangles, green inverted triangles, and blue squares are the distribution parameters calculated by Eq. (41) for steam-water two-phase flows under the pressures of 0.10, 1.0, 7.0, and 15 MPa, respectively. Fig. 9(b), (c), and 9(d) indicate that results from Eq. (41) agree with results from Eq. (15) within the data scatter indicated in Fig. 9(a). Thus, the prediction accuracy of Eq. (41) is considered to be similar to that of Eq. (15). Equation (41) allows for calculating the

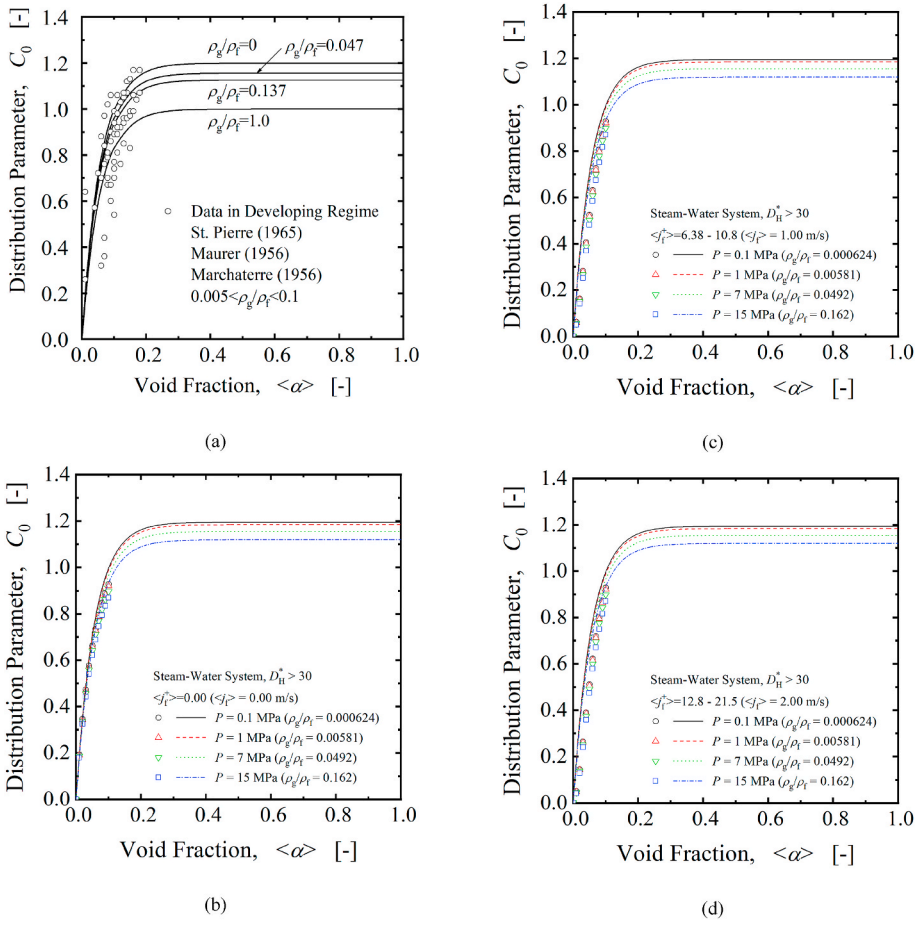

Fig. 9. Distribution parameter for subcooled boiling flows. Comparison of Ishii's correlation with: data (a); approximated correlation for $\langle j_f \rangle$ = 0.00 m/s (b); approximated correlation for $\langle j_f \rangle$ = 1.0 m/s (c); and approximated correlation for $\langle j_f \rangle$ = 2.0 m/s (d).

Table 2
Equation set of new drift-flux correlation applicable to dispersed two-phase flows in medium-to-large-size channels.

Drift-flux Model
$\langle\langle v_g^+ \rangle\rangle = C_0 \langle j^+ \rangle + \langle\langle v_{gj}^+ \rangle\rangle$.
Distribution Parameter
Adiabatic flow:
$C_0 = \{1.0e^{-60.63\langle\alpha_{KI}\rangle^{2.367}} + 1.2(1 - e^{-60.63\langle\alpha_{KI}\rangle^{2.367}})\} - \{1.0e^{-60.63\langle\alpha_{KI}\rangle^{2.367}} + 1.2(1 - e^{-60.63\langle\alpha_{KI}\rangle^{2.367}}) - 1\}N_\rho^{0.5}$,
where $\langle\alpha_{KI}\rangle = \dfrac{\langle j_g^+ \rangle}{C_0\langle j^+ \rangle + \langle\langle v_{gj,KI}^+ \rangle\rangle}$.
Saturated boiling flow:
$C_0 = 1.2 - 0.2N_\rho^{0.5}$.
Subcooled boiling flow:
$C_0 = (1.2 - 0.2N_\rho^{0.5})(1 - e^{-18\langle\alpha_{CT}\rangle})$,
where $\langle\alpha_{CT}\rangle = \dfrac{\langle j_g^+ \rangle}{C_0\langle j^+ \rangle + \sqrt{2}}$.
Drift Velocity
$\langle\langle v_{gj}^+ \rangle\rangle = \sqrt{2}(1 - \langle\alpha_{KI}\rangle)^{1.75} e^{-60.63\langle\alpha_{KI}\rangle^{2.367}} + \langle\langle v_{gj,KI}^+ \rangle\rangle(1 - e^{-60.63\langle\alpha_{KI}\rangle^{2.367}})$,
where $\langle\alpha_{KI}\rangle = \dfrac{\langle j_g^+ \rangle}{C_0\langle j^+ \rangle + \langle\langle v_{gj,KI}^+ \rangle\rangle}$.
Low viscosity systems ($N_{\mu f} \leq 2 \times 10^{-3}$):
$\langle\langle v_{gj,KI}^+ \rangle\rangle = 0.0019 D_H^{*\,0.809} N_\rho^{-0.157} N_{\mu f}^{-0.562}$ for $D_H^* \leq 30$
$\langle\langle v_{gj,KI}^+ \rangle\rangle = 0.030 N_\rho^{-0.157} N_{\mu f}^{-0.562}$ for $D_H^* \geq 30$
High viscosity systems ($N_{\mu f} \geq 2 \times 10^{-3}$):
$\langle\langle v_{gj,KI}^+ \rangle\rangle = 0.92 N_\rho^{-0.157}$ for $D_H^* \geq 30$.

distribution parameter for subcooled boiling flows with operating conditions explicitly. The equation set of the new drift-flux correlation is summarized in Table 2.

4.6. Distribution parameter for adiabatic bubbly flows

The distribution parameter for adiabatic bubbly flows in a round tube is given by Eq. (16). The parameter modeled by this equation is a function of bubble Sauter mean diameter. The bubble Sauter mean diameter depends on operating conditions $\langle j_g \rangle$ and $\langle j_f \rangle$. Thus, the distribution parameter modeled by Eq. (16) is an implicit function of operating conditions $\langle j_g \rangle$ and $\langle j_f \rangle$. Hibiki and Ishii (2002a) demonstrated that the distribution parameter for adiabatic bubbly flows in medium-size round tubes changes from about 0.9 to 1.2 as the void fraction increases. Motivation for developing a simple distribution parameter model leads to approximation of Eq. (16) as:

$$C_0 = \left\{1.0e^{-60.63\langle\alpha_{KI}\rangle^{2.367}} + 1.2\left(1 - e^{-60.63\langle\alpha_{KI}\rangle^{2.367}}\right)\right\} - \left\{1.0e^{-60.63\langle\alpha_{KI}\rangle^{2.367}} + 1.2\left(1 - e^{-60.63\langle\alpha_{KI}\rangle^{2.367}}\right) - 1\right\}N_\rho^{0.5} \quad (43)$$

The maximum difference in the calculated distribution parameter at the limit of $\langle\alpha\rangle = 0$ is a 20% between Eqs. (14) and (43). At the limit of $\langle\alpha\rangle = 0$, $C_0\langle j^+ \rangle$ is comparable to $\langle\langle v_{gj}^+ \rangle\rangle$ or negligibly smaller than $\langle\langle v_{gj}^+ \rangle\rangle$. Thus, the application of Eq. (14) to all dispersed two-phase flows, including bubbly flow, may not produce a significant prediction error of void fraction.

5. Validation of new drift-flux correlation with drift velocity model at the transition between bubbly and beyond-bubbly flows

5.1. Validation using data collected for atmospheric pressure conditions

This section demonstrates the validation of the new drift-flux correlation Eqs. (14) and (40) using the data collected for atmospheric pressure conditions. Four statistical parameters are introduced here to discuss the prediction accuracy.

Mean absolute error m_d

$$m_d = \frac{1}{N}\sum_{i=1}^{N}\left(\psi_{i,cal.} - \psi_{i,exp.}\right) \tag{44}$$

Standard deviation s_d

$$s_d = \sqrt{\frac{1}{N-1}\sum_{i=1}^{N}\left(\psi_{i,cal.} - \psi_{i,exp.} - m_d\right)^2} \tag{45}$$

Mean relative error m_{rel}

$$m_{rel} = \frac{1}{N}\sum_{i=1}^{N}\left(\frac{\psi_{i,cal.} - \psi_{i,exp.}}{\psi_{i,exp.}}\right) \tag{46}$$

Standard relative deviation s_{rel}

$$s_{rel} = \sqrt{\frac{1}{N-1}\sum_{i=1}^{N}\left(\frac{\psi_{i,cal.} - \psi_{i,exp.}}{\psi_{i,exp.}} - m_{rel}\right)^2} \tag{47}$$

Here N, $\psi_{i,cal.}$, and $\psi_{i,exp.}$ are the number of data, calculated value for the flow condition of the ith-datum, and experimental value for the ith-datum, respectively.

The mean absolute error m_d and mean relative error m_{rel} are the indices to describe the bias of an equation. Positive and negative values indicate the tendency of overestimation and underestimation, respectively. The standard deviation s_d and standard relative deviation s_{rel} are the indices to describe the random error of an equation. Large values indicate the tendency to scatter around the predicted value.

5.1.1. Validation using the database of Hibiki and Ishii (2000a)

Fig. 3(a) compares the new drift-flux correlation of Eqs. (14) and (40) with the data collected for nitrogen-water two-phase flows in a 0.102 m diameter round tube. A series of data were collected by changing superficial liquid velocity at a preset superficial gas velocity. The increase in mixture volumetric flux at the preset superficial gas velocity corresponds to the decrease in void fraction. Thin lines indicate the gas velocities predicted by the new drift-flux correlation. Thick black solid, red dashed, green dotted, and blue chain lines are the gas velocities predicted by Ishii's correlation for bubbly flow at $\langle\alpha\rangle = 0.3$, Ishii's correlation for bubbly flow at $\langle\alpha\rangle = 0.0$ or churn flow, Ishii's correlation for slug flow, and Kataoka and Ishii's correlation, respectively. The thick black line shows the lowest bound of the gas velocity.

For low superficial gas velocity conditions, the data are distributed along the line presented by Ishii's correlation for bubbly flow at a low void fraction. As the superficial gas velocity increases, the gas velocity increases and exceeds the value for slug flow. Finally, the gas velocity reaches the value predicted by Kataoka and Ishii's correlation.

Since the data are used to develop the new drift-flux correlation, it is no surprise that the new drift-flux correlation can reproduce the evolving process of the drift velocity well. However, the excellent agreement between the prediction and data demonstrates the validity of the modeling concept, Eqs. (37) and (38). Fig. 3(b) shows the prediction accuracy presented by $\langle\alpha_{cal.}\rangle/\langle\alpha_{exp.}\rangle$ against the measured void fraction $\langle\alpha_{exp.}\rangle$. No noticeable and systematic prediction error is observed between $\langle\alpha_{exp.}\rangle = 0.0910$ and 0.341. The values of the statistical indices are

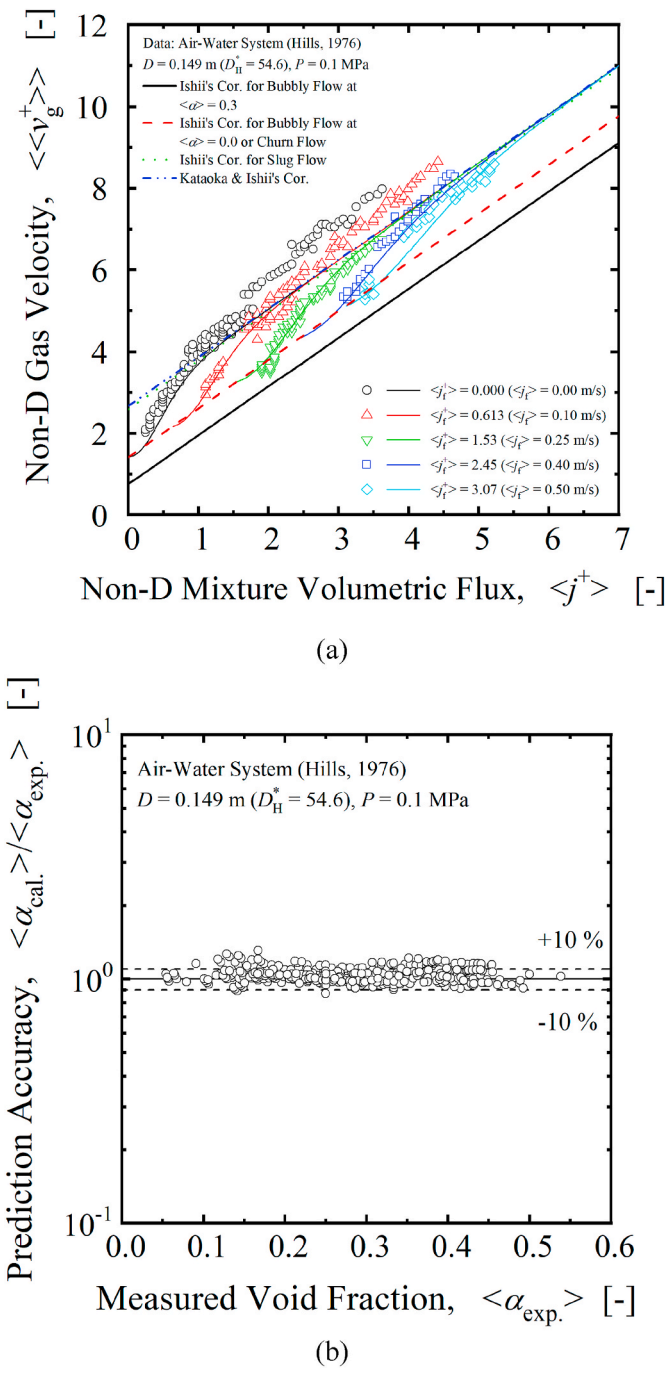

Fig. 10. Drift-flux plot (a) and new drift-flux correlation performance (b). The database of Hills, (1976) was used.

$m_d = 1.80 \times 10^{-6}$, $s_d = 0.00664$, $m_{rel} = -0.00188$, and $m_{rel,ab} = 0.0347$.

5.1.2. Validation using the database of Hills (1976)

Fig. 10(a) compares the new drift-flux correlation of Eqs. (14) and (40) with the low flow data collected for air-water two-phase flows in a 0.149 m diameter round tube. Fig. 4 shows the drift-flux plot for the high flow data. A series of data were collected by changing superficial gas velocity at a preset superficial liquid velocity. The increase in mixture volumetric flux at the preset superficial liquid velocity corresponds to the increase in void fraction. Thin lines indicate the gas velocities predicted by the new drift-flux correlation. For low superficial gas velocity conditions, the data are distributed along the line presented by Ishii's correlation for bubbly flow at a low void fraction. Some data for $\langle j_f^+\rangle =$

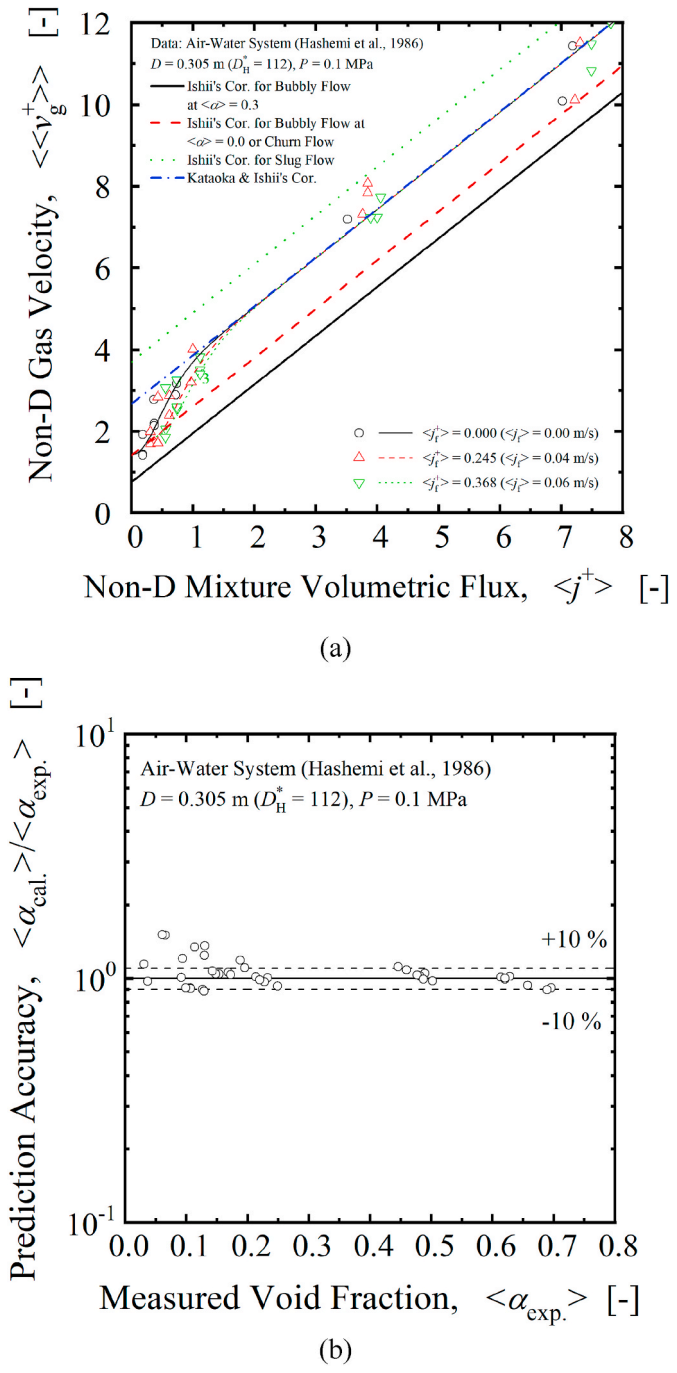

Fig. 11. Drift-flux plot (a) and new drift-flux correlation performance (b). The database of Hashemi et al. (1986) was used.

1.53 and 3.07 appear below the line of Ishii's correlation for bubbly flow at $\langle\alpha\rangle = 0$. The data smaller than the thick red dashed line indicate that the increase in void fraction decreases the drift velocity, as shown in Eq. (9). As the superficial gas velocity further increases, the drift velocity increases. Finally, the drift velocity reaches the value predicted by Kataoka and Ishii's correlation. The data follow the lines predicted by the new drift-flux correlation.

The new drift-flux correlation tends to underestimate the gas velocity for $\langle j^+\rangle \geq 1.5$ for the pool data with $\langle j_f^+\rangle = 0$. The discontinuity of the data indicated by black circles appears around $\langle j^+\rangle = 1.5$. In the region of $\langle j^+\rangle \geq 1.5$, the new drift-flux correlation is reduced to Kataoka and Ishii's correlation, which has been validated by extensive existing pool void fraction data. There is a possibility that the deviation between the new drift-flux correlation and pool data for $\langle j^+\rangle \geq 1.5$ is due to the measurement uncertainty. The deviation is within a 10% range. Thus, the new drift-flux correlation is still valid for the pool data.

Although the data are not used to develop the new drift-flux correlation, the new drift-flux correlation can reproduce the evolving process of the drift velocity well. The excellent agreement between the prediction and data demonstrates the validity of the modeling concept, Eqs. (37) and (38). Fig. 10(b) shows the prediction accuracy presented by $\langle\alpha_{cal.}\rangle/\langle\alpha_{exp.}\rangle$ against the measured void fraction $\langle\alpha_{exp.}\rangle$. No noticeable and systematic prediction error for the low and high flow data is observed between $\langle\alpha_{exp.}\rangle = 0.0539$ and 0.538. The values of the statistical indices for the low flow data are $m_d = 0.0161$, $s_d = 0.0206$, $m_{rel} = 0.0553$, and $s_{rel} = 0.0665$. The values of the statistical indices for the high flow data are $m_d = -0.00313$, $s_d = 0.0196$, $m_{rel} = -0.00398$, and $s_{rel} = 0.0642$.

5.1.3. Validation using the database of Hashemi et al. (1986)

Fig. 11(a) compares the new drift-flux correlation of Eqs. (14) and (40) with the data collected for air-water two-phase flows in a 0.305 m diameter round tube. A series of data were collected by changing superficial gas velocity at a preset superficial liquid velocity. Thin lines indicate the gas velocities predicted by the new drift-flux correlation. For low superficial gas velocity conditions, the data are distributed along the line presented by Ishii's correlation for bubbly flow at a low void fraction. Some data also appear below the line of Ishii's correlation for bubbly flow at $\langle\alpha\rangle = 0$. The data smaller than the thick red dashed line indicate that the increase in void fraction decreases the drift velocity, as shown in Eq. (9). As the superficial gas velocity further increases, the drift velocity increases. Finally, the drift velocity reaches the value predicted by Kataoka and Ishii's correlation. The data follow the lines predicted by the new drift-flux correlation. Due to the large-size channel ($D = 0.305$ m), the gas velocity calculated by Ishii's correlation for slug flow is higher than that by Kataoka and Ishii's correlation. As expected, Ishii's correlation for slug flow overpredicts the gas velocity.

Although the data are not used to develop the new drift-flux correlation, the new drift-flux correlation can reproduce the evolving process of the drift velocity well. The excellent agreement between the prediction and data demonstrates the validity of the modeling concept, Eqs. (37) and (38). Fig. 11(b) shows the prediction accuracy presented by $\langle\alpha_{cal.}\rangle/\langle\alpha_{exp.}\rangle$ against the measured void fraction $\langle\alpha_{exp.}\rangle$. No noticeable and systematic prediction error except for some low void fraction data is observed between $\langle\alpha_{exp.}\rangle = 0.0305$ and 0.696. It should be noted here that the deterioration of the prediction accuracy defined by $\langle\alpha_{cal.}\rangle/\langle\alpha_{exp.}\rangle$ is over-magnified at low void fractions, and the measurement accuracy of a single gamma densitometer may also deteriorate at low void fractions. The values of the statistical indices are $m_d = 0.00457$, $s_d = 0.0253$, $m_{rel} = 0.0572$, and $s_{rel} = 0.153$.

5.1.4. Validation using the database of Schlegel et al. (2014)

Fig. 12(a), (b), and 12(c) compare the new drift-flux correlation of Eqs. (14) and (40) with the data collected for air-water two-phase flows in 0.152, 0.203, and 0.305 m diameter round tubes, respectively. The scale of the figures is expanded to show the low mixture volumetric flux range $\langle j^+\rangle \leq 30$. A series of data were collected by changing superficial gas velocity at a preset superficial liquid velocity. Thin lines indicate the gas velocities predicted by the new drift-flux correlation. For low superficial gas velocity conditions, the data are distributed along the line presented by Ishii's correlation for bubbly flow at a low void fraction. Some data also appear below the line of Ishii's correlation for bubbly flow at $\langle\alpha\rangle = 0$. The data smaller than the thick red dashed line indicate that the increase in void fraction decreases the drift velocity, as shown in Eq. (9). As the superficial gas velocity further increases, the drift velocity increases. Finally, the drift velocity reaches the value predicted by Kataoka and Ishii's correlation. The data follow the lines predicted by the new drift-flux correlation.

Although the data are not used to develop the new drift-flux corre-

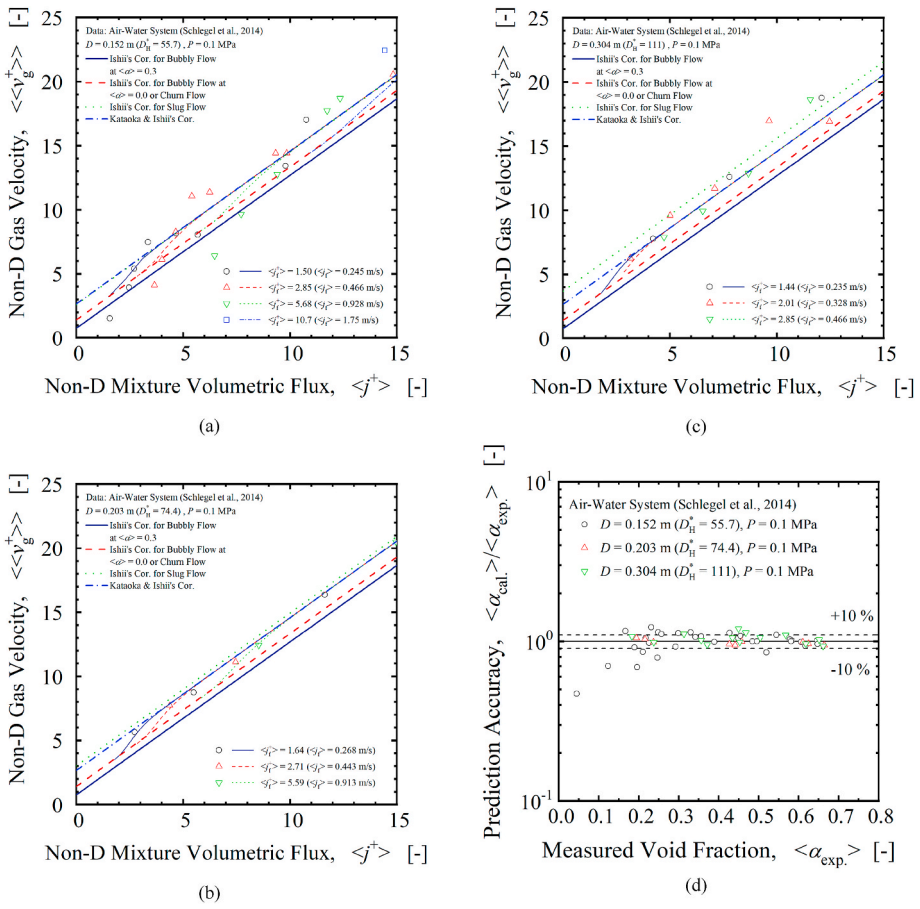

Fig. 12. Drift-flux plots (a)–(c) and new drift-flux correlation performance (d). The database of Schlegel et al. (2014) was used.

lation, the new drift-flux correlation can reproduce the evolving process of the drift velocity well. The excellent agreement between the prediction and data demonstrates the validity of the modeling concept, Eqs. (37) and (38). Fig. 12(d) shows the prediction accuracy presented by $\langle \alpha_{cal.} \rangle / \langle \alpha_{exp.} \rangle$ against the measured void fraction $\langle \alpha_{exp.} \rangle$. No noticeable and systematic prediction error except for some low void fraction data is observed between $\langle \alpha_{exp.} \rangle = 0.0447$ and 0.664. It should be noted here that the deterioration of the prediction accuracy defined by $\langle \alpha_{cal.} \rangle / \langle \alpha_{exp.} \rangle$ is over-magnified at low void fractions, and the measurement accuracy of a four-sensor probe may also deteriorate at low void fractions. The values of the statistical indices for the data collected in the 0.152 m diameter round tube are $m_d = 0.00307$, $s_d = 0.0341$, $m_{rel} = -0.0130$, and $s_{rel} = 0.156$. The values of the statistical indices for the data collected in the 0.203 m diameter round tube are $m_d = -0.00958$, $s_d = 0.0147$, $m_{rel} = -0.0128$, and $s_{rel} = 0.0351$. The values of the statistical indices for the data collected in the 0.304 m diameter round tube are $m_d = 0.0169$, $s_d = 0.0358$, $m_{rel} = 0.0422$, and $s_{rel} = 0.0758$.

5.1.5. *Validation using the database of Shen et al. (2015)*

Fig. 13(a) compares the new drift-flux correlation of Eqs. (14) and (40) with the low flow data collected for air-water two-phase flows in a 0.200 m diameter round tube. A series of data were collected by changing superficial gas velocity at a preset superficial liquid velocity. The increase in mixture volumetric flux at the preset superficial liquid velocity corresponds to the increase in void fraction. Thin lines indicate the gas velocities predicted by the new drift-flux correlation. For low superficial gas velocity conditions, the data are distributed along the line presented by Ishii's correlation for bubbly flow at a low void fraction. Some data appear below the line of Ishii's correlation for bubbly flow at $\langle \alpha \rangle = 0$. The data smaller than the thick red dashed line indicate that the increase in void fraction decreases the drift velocity, as shown in Eq. (9). As the superficial gas velocity further increases, the drift velocity increases. Finally, the drift velocity reaches the value predicted by Kataoka and Ishii's correlation. The data follow the lines predicted by the new drift-flux correlation.

The new drift-flux correlation tends to underestimate the gas velocity for $\langle j_f^+ \rangle = 0.308$ and $\langle j^+ \rangle \geq 2.5$. The flow condition is close to the pool conditions. In the pool conditions, the new drift-flux correlation is reduced to Kataoka and Ishii's correlation, which has been validated by extensive existing pool void fraction data. There is a possibility that the deviation between the new drift-flux correlation and pool data is due to the measurement uncertainty. Shen et al. pointed out that the increase in superficial gas velocity at the low superficial liquid velocity might induce complicated multi-dimensional flow behaviors. In such flow conditions, it might be difficult for the four-sensor probe placed against the axial flow direction to provide accurate measurements because bubbles may hit the probe from its downstream side. The complicated flow behaviors are suppressed by increasing superficial liquid velocity. The deviation is within a 20% range. Thus, the new drift-flux correlation is still valid for the pool data.

Although the data are not used to develop the new drift-flux correlation, the new drift-flux correlation can reproduce the evolving process of the drift velocity well. The excellent agreement between the prediction and data demonstrates the validity of the modeling concept, Eqs. (37) and (38). Fig. 13(b) shows the prediction accuracy presented by $\langle \alpha_{cal.} \rangle / \langle \alpha_{exp.} \rangle$ against the measured void fraction $\langle \alpha_{exp.} \rangle$. No noticeable and systematic prediction error is observed between $\langle \alpha_{exp.} \rangle = 0.0280$ and 0.406. The values of the statistical indices are $m_d = 0.00771$, $s_d = 0.0329$, $m_{rel} = 0.0175$, and $s_{rel} = 0.133$.

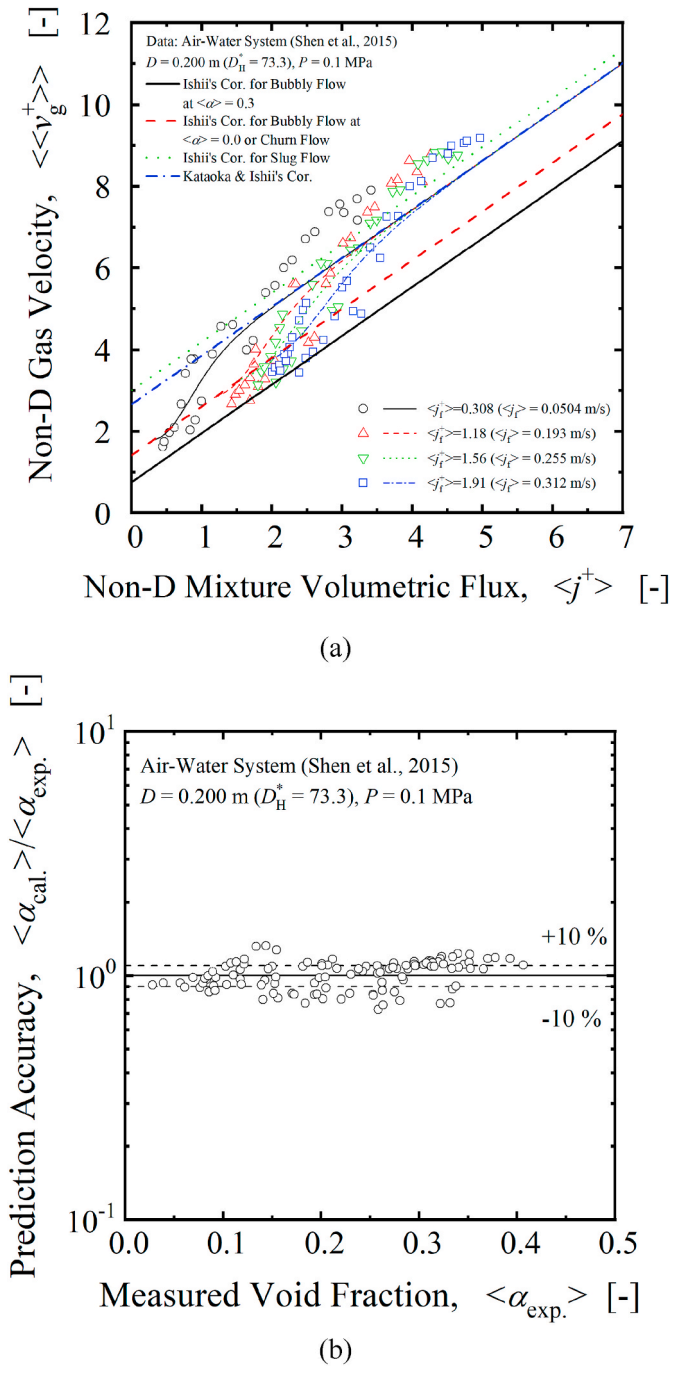

Fig. 13. Drift-flux plot (a) and new drift-flux correlation performance (b). The database of Shen et al. (2015) was used .

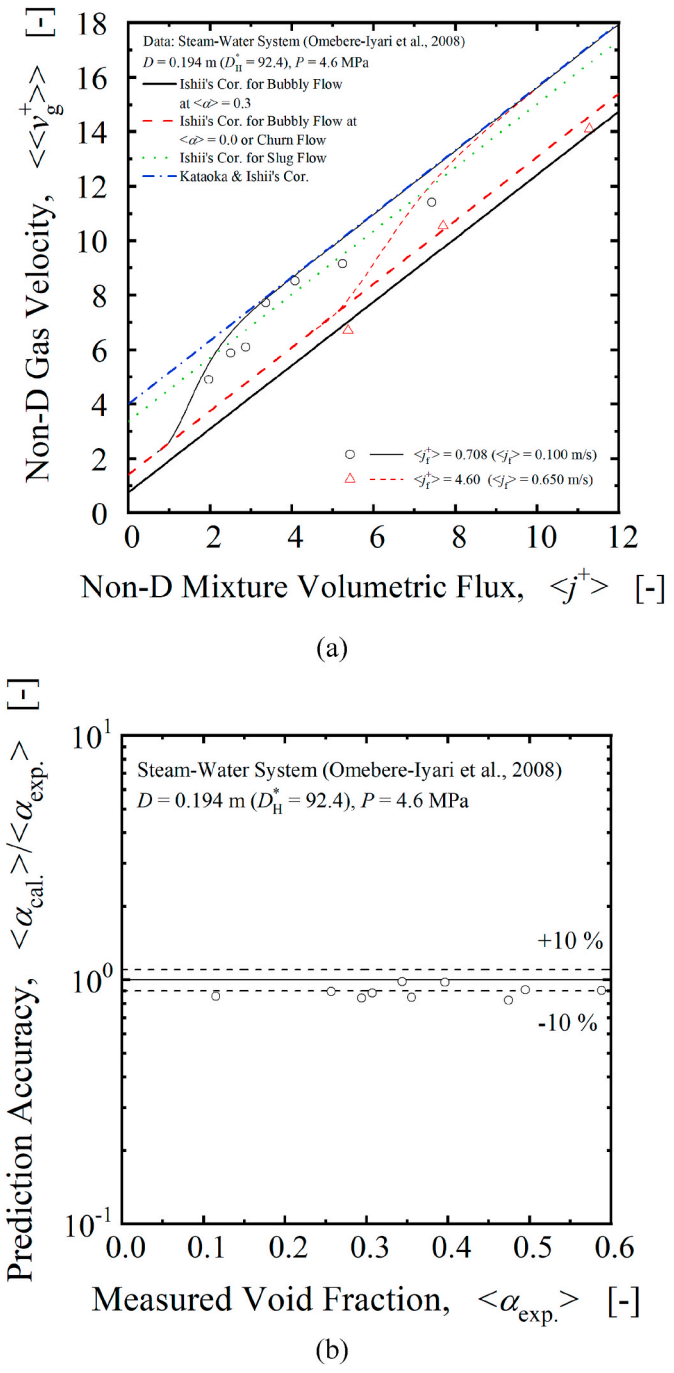

Fig. 14. Drift-flux plot (a) and new drift-flux correlation performance (b). The database of Omebere-Iyari et al. (2008) was used.

5.1.6. Validation using the database of Hsu et al. (1998)

Fig. 2(a) compares the new drift-flux correlation of Eqs. (14) and (40) with the data collected for nitrogen-water two-phase flows in a 0.0508 m diameter round tube. A series of data were collected by changing superficial liquid velocity at a preset superficial gas velocity. The increase in mixture volumetric flux at the preset superficial gas velocity corresponds to the decrease in void fraction. Thin lines indicate the gas velocities predicted by the new drift-flux correlation. For low superficial gas velocity conditions, some data appear below the line of Ishii's correlation for bubbly flow at $\langle\alpha\rangle = 0$. The data smaller than the thick red dashed line indicate that the increase in void fraction decreases the drift velocity, as shown in Eq. (9). As the superficial gas velocity increases, the drift velocity increases and, finally, the drift velocity reaches the values predicted by Ishii's correlation for slug flow or Kataoka and Ishii's correlation.

Although the data are not used for developing the new drift-flux correlation, the new drift-flux correlation can reproduce the evolving process of the drift velocity well. The excellent agreement between the prediction and data demonstrates the validity of the modeling concept, Eqs. (37) and (38). Fig. 2(b) shows the prediction accuracy presented by $\langle\alpha_{cal.}\rangle/\langle\alpha_{exp.}\rangle$ against the measured void fraction $\langle\alpha_{exp.}\rangle$. No noticeable and systematic prediction error is observed between $\langle\alpha_{exp.}\rangle = 0.130$ and 0.395. The values of the statistical indices are m_d = -0.00958, s_d = 0.0182, m_{rel} = -0.0260, and s_{rel} = 0.0810.

Table 3
Performance evaluation of new drift-flux correlation.

References	Gas Velocity, $<<v_g>>$				Void Fraction, $<\alpha>$			
	m_d	s_d	m_{rel}	$m_{rel,ab}$	m_d	s_d	m_{rel}	$m_{rel,ab}$
	[m/s]	[m/s]	[-]	[-]	[-]	[-]	[-]	[-]
Hsu et al. (1998)	0.132	0.342	0.0332	0.0814	−0.00958	0.0182	−0.0260	0.0810
Hibiki and Ishii, (2000a)	0.00395	0.126	0.00311	0.0360	1.80×10^{-6}	0.00664	−0.00188	0.0347
Hills, (1976) (Low flow)	−0.268	0.323	−0.0488	0.0587	0.0161	0.0206	0.0553	0.0665
Hills, (1976) (High flow)	0.397	1.11	0.00773	0.0590	−0.00313	0.0196	−0.00398	0.0642
Hashemi et al. (1986)	−0.109	0.458	−0.0377	0.118	0.00457	0.0253	0.0572	0.153
Schlegel et al. (2014) (6 inch diameter)	−0.306	1.60	0.0491	0.246	0.00307	0.0341	−0.0130	0.156
Schlegel et al. (2014) (8 inch diameter)	0.338	0.529	0.0140	0.0355	−0.00958	0.0147	−0.0128	0.0351
Schlegel et al. (2014) (12 inch diameter)	−0.506	1.15	−0.0359	0.0687	0.0169	0.0358	0.0422	0.0758
Shen et al. (2015)	−0.178	0.663	0.000570	0.139	0.00771	0.0329	0.0175	0.133
Omebere-Iyari et al. (2008)	1.11	0.858	0.126	0.0667	−0.0383	0.0241	−0.109	0.0576
Kawanishi et al. (1990)	0.897	1.44	0.0736	0.141	N/A	N/A	N/A	N/A
Average value	−0.0561	0.779	−0.0123	0.104	0.00689	0.0254	0.0250	0.0964

5.2. Validation using data collected for high-pressure conditions

This section demonstrates the validation of the new drift-flux correlation of Eqs. (14) and (40) using the data collected for high-pressure conditions.

5.2.1. Validation using the database of Omebere-Iyari et al. (2008)

Fig. 14(a) compares the new drift-flux correlation of Eqs. (14) and (40) with the data collected for steam-water two-phase flows in a 0.194 m diameter round tube at the pressure of 4.6 MPa. A series of data were collected by changing superficial gas velocity at a preset superficial liquid velocity. The increase in mixture volumetric flux at the preset superficial liquid velocity corresponds to the increase in void fraction. Thin lines indicate the gas velocities predicted by the new drift-flux correlation. The drift velocity for $\langle j_f^+ \rangle = 0.708$ increases gradually and reaches a constant value as the superficial gas velocity increases. The gas velocity data for $\langle j_f^+ \rangle = 4.60$ are lower than those for $\langle j_f^+ \rangle = 0.708$. The void fractions measured for $\langle j_f^+ \rangle = 0.708$ and 4.60 at similar $\langle j^+ \rangle$ (~7.5) are 0.588 and 0.474, respectively, and the difference is 25%. Omebere-Iyari et al. measured the void fraction distribution along the tube radius. The measurement values indicate the void fraction distribution for $\langle j_f^+ \rangle = 4.60$ is much flatter than that for $\langle j_f^+ \rangle = 0.708$. Thus, the distribution parameter for $\langle j_f^+ \rangle = 4.60$ is lower than that for $\langle j_f^+ \rangle = 0.708$. The lowered gas velocity observed for $\langle j_f^+ \rangle = 4.60$ is due to the lowered distribution parameter. The flatter void fraction distribution may be due to the unique gas injection method which Omebere-Iyari et al. used: they injected the gas phase from the channel wall, whereas other investigators injected the gas phase uniformly. The effect of injection method might not be negligible for higher superficial liquid velocity conditions $\langle j_f^+ \rangle = 4.60$.

Although the data are not used for developing the new drift-flux correlation, the new drift-flux correlation can reasonably reproduce the evolving process of the drift velocity. The good agreement between the prediction and data demonstrates the validity of the modeling concept, Eqs. (37) and (38). Fig. 14(b) shows the prediction accuracy presented by $\langle \alpha_{cal.} \rangle / \langle \alpha_{exp.} \rangle$ against the measured void fraction $\langle \alpha_{exp.} \rangle$. The new drift-flux correlation tends to slightly underestimate the measured void fraction data due probably to the unique gas injection method. The values of the statistical indices are m_d = -0.0383, s_d = 0.0241, m_{rel} = -0.109, and s_{rel} = 0.0576.

5.2.2. Validation using the database of Kawanishi et al. (1990)

Kawanishi et al. measured void fraction for steam-water two-phase flows in a 0.102 m diameter round tube at the pressure of 1.5 MPa. Their database did not provide complete sets of data for each data point, namely $\langle j_g \rangle$, $\langle j_f \rangle$, and $\langle \alpha \rangle$. However, the data are important to examine the applicability of Kataoka and Ishii's correlation to high-pressure steam-water two-phase flows in the large-size channel. Fig. 5(a) compares Kataoka and Ishii's correlation with the data. Fig. 5(b) shows the prediction accuracy presented by $\langle\langle v_{g,cal.}^+ \rangle\rangle / \langle\langle v_{g,exp.}^+ \rangle\rangle$ against the measured gas velocity $\langle\langle v_{g,exp.}^+ \rangle\rangle$. No noticeable and systematic prediction error except for some low gas velocity data is observed between $\langle\langle v_{g,exp.}^+ \rangle\rangle = 4.14$ and 32.4. The values of the statistical indices for the gas velocity data are $m_d = 0.897$ m/s, $s_d = 1.44$ m/s, $m_{rel} = 0.0736$, and $s_{rel} = 0.141$.

6. Conclusion

The drift-flux model plays a critical role in two-phase flow numerical simulations for heat transfer analyses. The drift-flux model is characterized by two drift-flux parameters: distribution parameter and drift velocity. The distribution parameter represents the covariance effect of the distributions for void fraction and mixture volumetric flux. In addition to the physical properties of a two-phase system, channel geometry may be the most influential parameter affecting the distribution parameter. Providing the channel geometry and physical properties are the same, the distribution parameter is almost constant except for subcooled boiling flow and annular flow conditions. The drift velocity represents the relative velocity between gas and liquid phases. In addition to the physical properties of a two-phase system, channel size and flow regime may be the most influential parameters affecting the drift velocity.

The present study aimed at developing a comprehensive and robust drift velocity model for dispersed two-phase flows in medium-to-large-size channels. The key was to model the behavior of the drift velocity at the transition between bubbly and beyond-bubbly flows. The mechanistic two-group approach was introduced to develop the basic concept of the drift velocity model. The drift velocity model, taking the flow regime transition into account, was developed by approximating the two-group approach.

The new drift-flux correlation with the drift velocity model was extensively evaluated using 750 data collected from eight different sources. The fluid systems were nitrogen-water, air-water, and steam-water systems. The flow channel diameter ranged from 0.0508 to 0.305 m. The test section height-to-channel diameter L/D ranged from 9.41 to 130. The superficial gas velocity was changed from 0.0100 to 11.2 m/s, whereas the superficial liquid velocity was changed from 0 to 2.6 m/s. The operating pressure covered the range from 0.1 to 4.6 MPa.

As summarized in Table 3, the values of the statistical indices for void fraction were m_d = 0.00689, s_d = 0.0254, m_{rel} = 0.0250, and s_{rel} = 0.0964. The prediction bias of the new drift-flux correlation was negligibly small, and the random error was about 3% in an absolute value measure and 10% in a relative value measure. The values of the statistical indices for gas velocity were m_d = -0.0561 m/s, s_d = 0.779 m/s, m_{rel}

= -0.0123, and s_{rel} = 0.104. The prediction bias of the new drift-flux correlation was negligibly small, and the random error was about 10% in a relative value measure. The above extensive evaluation results demonstrated the validity of the new drift-flux correlation for a wide range of test conditions, including the pressure from 0.1 to 4.6 MPa and round tube diameter up to 0.305 m. The major advantages of the new drift flux correlation developed here are summarized below.

- The new drift-flux correlation was applicable to entire dispersed two-phase flow conditions, including flow regime transition conditions.
- The new drift-flux correlation was applicable to medium-to-large round tubes, which cover the diameter range important in industrial piping systems.
- The new drift-flux correlation was applicable to a wide range of thermal-fluid conditions, including high-pressure conditions up to 4.6 MPa.
- The new drift-flux correlation was explicit for operating conditions, such as $\langle j_g \rangle$ and $\langle j_f \rangle$.

The new drift-flux correlation is simple enough to be implemented into existing one-dimensional computational codes without any substantial code architecture change.

Declaration of competing interest

The authors declare the following financial interests/personal relationships which may be considered as potential competing interests: Takashi Hibiki reports article publishing charges and travel were provided by Nuclear Regulation Authority. Takashi Hibiki reports a relationship with Nuclear Regulation Authority that includes: funding grants.

Data availability

The authors do not have permission to share data.

Acknowledgment

This work was performed under the auspices of the Secretariat of the Nuclear Regulation Authority of Japan. One of the authors (T. Hibiki) would like to express his sincere appreciation to the Secretariat and to the Hong Kong SAR government for supporting his research under the Global STEM Professorship.

References

Andersen, J.G.M., Chu, K.H., 1983. BWR Refill-Reflood Program Constitutive Correlations for Shear and Heat Transfer for the BWR Version of TRAC, NUREG.CR-2134.
ANSYS, 2017. ANSYS Fluent Theory Guide.
Baily, R.v., Zmola, P.C., Taylor, F.M., Planchet, R.J., 1956. Transport of gases through liquid-gas mixture. In: AIChE New Orleans Meeting. New Orleans, USA.
Borkowski, J.A., Wade, W., 1992. TRAC-BF1/MOD1 Models and Correlations. US NRC, Washington DC. NUREG/CR-4391/EGG-26804.
Brooks, C.S., Hibiki, T., Ishii, M., 2012a. Interfacial drag force in one-dimensional two-fluid model. Prog. Nucl. Energy 61, 57–68.
Brooks, C.S., Paranjape, S.S., Ozar, B., Hibiki, T., Ishii, M., 2012b. Two-group drift-flux model for closure of the modified two-fluid model. Int. J. Heat Fluid Flow 37, 196–208.
Carver, M.B., Carlucci, L.N., Inch, W.W.R., 1981. Thermal-hydraulics in Recirculating Steam Generators - THIRST Code User's Manual. Atomic Energy Can Ltd AECL Rep.
Clark, N., Flemmer, R., 1986. The effect of varying gas voidage distributions on average holdup in vertical bubble flow. Int. J. Multiphas. Flow 12, 299–302.
Clark, N.N., Flemmer, R.L., 1985. Predicting the holdup in two-phase bubble upflow and downflow using the Zuber and Findlay drift-flux model. AIChE J. 31, 500–503.
Hashemi, A., Kim, J.H., Sursock, J.P., 1986. Effect of diameter and geometry on two-phase flow regimes and carry-over in a model PWR hot leg. In: 8th International Heat Transfer Conference, pp. 2443–2451. San Francisco, CA, USA.
Hibiki, T., 2019. One-dimensional drift-flux correlations for two-phase flow in medium-size channels. Exp Comput Multiph Flow 1, 85–100.
Hibiki, T., Ishii, M., 2003. One-dimensional drift–flux model for two-phase flow in a large diameter pipe. Int. J. Heat Mass Tran. 46, 1773–1790.
Hibiki, T., Ishii, M., 2002a. Distribution parameter and drift velocity of drift-flux model in bubbly flow. Int. J. Heat Mass Tran. 45, 707–721.
Hibiki, T., Ishii, M., 2002b. Interfacial area concentration of bubbly flow systems. Chem. Eng. Sci. 57, 3967–3977.
Hibiki, T., Ishii, M., 2000a. Experimental study on hot-leg U-bend two-phase natural circulation in a loop with a large diameter pipe. Nucl. Eng. Des. 195, 69–84.
Hibiki, T., Ishii, M., 2000b. Two-group interfacial area transport equations at bubbly-to-slug flow transition. Nucl. Eng. Des. 202, 39–76.
Hibiki, T., Ishii, M., 1999. Experimental study on interfacial area transport in bubbly two-phase flows. Int. J. Heat Mass Tran. 42, 3019–3035.
Hibiki, T., Ishii, M., Xiao, Z., 2001. Axial interfacial area transport of vertical bubbly flows. Int. J. Heat Mass Tran. 44, 1869–1888.
Hibiki, T., Ju, P., Rassame, S., Miwa, S., Shen, X., Ozaki, T., 2022. Channel size effect on drift-flux parameters for adiabatic and boiling two-phase flows. Int. J. Heat Mass Tran. 185, 122410.
Hibiki, T., Saito, Y., Mishima, K., Tobita, Y., Konishi, K., Matsubayashi, M., 2000. Study on flow characteristics in gas-molten metal mixture pool. Nucl. Eng. Des. 196, 233–245.
Hills, J.H., 1976. The operation of a bubble column at high throughputs: I. Gas holdup measurement. Chem. Eng. J. 12, 89–99.
Hotta, A., Zhang, M., Shirai, H., 2004. Application of TRAC/BF1-ENTRÉE-NASCA to OECD NEA/NSC BWR turbine trip benchmark. Nucl. Sci. Eng. 148, 208–225.
Hsu, J.-T., Ishii, M., Hibiki, T., 1998. Experimental study on two-phase natural circulation and flow termination in a loop. Nucl. Eng. Des. 186, 395–409.
Ishii, M., 1977. One-dimensional Drift-Flux Model and Constitutive Equations for Relative Motion between Phases in Various Two-phase Flow Regimes. ANL, p. 77, 47.
Ishii, M., Hibiki, T., 2011. Thermo-Fluid Dynamics of Two-phase Flow, second ed.
Kataoka, I., Ishii, M., 1987. Drift flux model for large diameter pipe and new correlation for pool void fraction. Int. J. Heat Mass Tran. 30, 1927–1939.
Kawanishi, K., Hirao, Y., Tsuge, A., 1990. An experimental study on drift flux parameters for two-phase flow in vertical round tubes. Nucl. Eng. Des. 120, 447–458.
Khan, I., Wang, M., Zhng, Y., Tian, W., Su, G., Qiu, S., 2000. Two-phase bubbly flow simulation using CFD method: a review of models for interfacial forces. Prog. Nucl. Energy 125, 103360.
Kitscha, J., Kocamustafaogullari, G., 1989. Breakup criteria for fluid particles. Int. J. Multiphas. Flow 15, 573–588.
Kocamustafaogullari, G., Ishii, M., 1985. Maximum fluid particle size for bubbles and drops. Fed. Times vol. 29, 99–107. ASME Winter Annual Meeting, Proceedings of Fundamental Aspects of Gas-Liquid Flow.
Komuro, Y., Kodama, A., Kondoh, Y., Azuma, S., Morita, H., Tanimoto, K., Kawakami, R., Taguchi, K., Hibiki, T., 2022. Validation of three-dimensional simulation method for two-phase flow in triangular-pitch tube bundle in secondary side of steam generators on porous two-fluid model. J. Nucl. Sci. Technol. 59, 78–95.
Marchaterre, J.F., 1956. The Effect of Pressure on Boiling Density in Multiple Rectangular Channels. ANL-5522.
Maurer, G.W., 1956. A Method of Predicting Steady State Boiling Vapour Fractions in Reactor Coolant Channels, vol. 19. WAPD-BT.
Moorthi, A., Kumar Sharma, A., Velusamy, K., 2018. A review of sub-channel thermal hydraulic codes for nuclear reactor core and future directions. Nucl. Eng. Des. 332, 329–344.
Nuclear Regulatory Committee, U.S., 2008. TRACE V5.0 Theory Manual. Field Equations, Solutions Methods, and Physical Models.
Omebere-Iyari, N.K., Azzopardi, B.J., Lucas, D., Beyer, M., Prasser, H.M., 2008. The characteristics of gas/liquid flow in large risers at high pressures. Int. J. Multiphas. Flow 34, 461–476.
Salko, R., Avramova, M., Wysoski, A., Toptan, A., Hu, J., Porter, N., Blyth, T., Dances, C., Gomez, A., Jernigan, C., Kelly, J., 2019. CTF Theory Manual.
Schlegel, J.P., Sharma, S., Cuenca, R.M., Hibiki, T., Ishii, M., 2014. Local flow structure beyond bubbly flow in large diameter channels. Int. J. Heat Fluid Flow 47, 42–56.
Sharma, Subash L., Hibiki, T., Ishii, M., Brooks, C.S., Schlegel, J.P., Liu, Y., Buchanan Jr., J.R., 2017a. Turbulence-induced bubble collision force modeling and validation in adiabatic two-phase flow using CFD. Nucl. Eng. Des. 312, 399–409.
Sharma, S.L., Hibiki, T., Ishii, M., Schlegel, J.P., Buchanan Jr., J.R., Hogan, K.J., Guilbert, P.W., 2017b. An interfacial shear term evaluation study for adiabatic dispersed air-water two-phase flow with the two-fluid model using CFD. Nucl. Eng. Des. 312, 389–398.
Shen, X., Hibiki, T., Nakamura, H., 2015. Bubbly-to-cap bubbly flow transition in a long-26 m vertical large diameter pipe at low liquid flow rate. Int. J. Heat Fluid Flow 52, 140–155.
Shipley, D.G., 1984. Two phase flow in large diameter pipes. Chem. Eng. Sci. 39, 163–165.
Singhal, A.K., Keeton, L.W., Spalding, D.B., Srikantiah, G.S., 1982. ATHOS: a computer program for thermal-hydraulic analysis of steam generators. Mathematical and Physical Models and Method of Solution ume 1. EPRI-NP-2698-CCM.
St Pierre, C.C., 1965. Frequency-response Analysis of Steam Voids to Sinusoidal Power Modulation in a Thin-Walled Boiling Water Coolant Channel. Argonne National Laboratory. ANL-7041.
Thermal Hydraulics Group, 1998. RELAP5/MOD3 Code Manual. Vol. 1: Code Structure, System Models and Solution Methods. NUREG/CR-5535/Rev 1.
Yeoh, G.H., 2019. Thermal hydraulic considerations of nuclear reactor systems: past, present and future challenges. Exp Comput Multiph Flow 1, 3–27.
Zuber, N., Findlay, J.A., 1965. Average volumetric concentration in two-phase flow systems. J. Heat Tran. 87, 453–468.